UC San Diego
UC San Diego Electronic Theses and Dissertations

Title

Role of the Lung Microenvironment in Regulating Adult and Neonatal AM Transcriptional Activity

Permalink

https://escholarship.org/uc/item/9fq1p70k

Author

Yamamura, Asami

Publication Date

2020

Peer reviewed|Thesis/dissertation

UNIVERSITY OF CALIFORNIA SAN DIEGO

Role of the Lung Microenvironment in Regulating Adult and Neonatal AM Transcriptional
Activity

A Dissertation Submitted in Partial Satisfaction of the Requirements for the Degree

Doctor of Philosophy

in

Biomedical Sciences

by

Asami Yamamura

Committee in charge:

      Professor Lawrence Prince, Chair
      Professor Christopher Glass
      Professor Yury Miller
      Professor Stephen Spector
      Professor David Traver

2020

The Dissertation of Asami Yamamura is approved and it is acceptable in quality and form for publication on microfilm and electronically:

_____

_____

_____

_____
Chair

University of California San Diego

2020

DEDICATION

I would like to dedicate this dissertation to my parents, husband, and baby boy for their love and support.

TABLE OF CONTENTS

LIST OF ABBREVIATIONS

AGM	Aorta-gonads-mesonephros
AIM2	Absent in melanoma 2
AM	Alveolar macrophages
AP-1	Activator protein 1
ATAC-seq	Assay for transposase-accessible chromatin
Bach2	B lymphoid transcription repressor BTB and CNC homology 2
BM	Bone marrow
BPD	Bronchopulmonary dysplasia
CD	Cluster of differentiation
C/EBP	CCAAT-enhancer-binding proteins
CPM	Counts per million
E	Embryonic day
E. coli	*Escherichia coli*
FACS	Fluorescence-activated cell sorting
FC	Fold change
GATA	GATA-binding factor
GBS	Group B *Streptococcus*
GM-CSF	Granulocyte-macrophage colony-stimulating factor
h	Hour
HIF	Hypoxia-inducible transcription factors
IDR	Irreproducibility discovery rate

IL	Interleukin
I.n.	Intranasal
IM	Interstitial macrophage
IPA	Ingenuity pathway analysis
IRF	Interferon regulatory factor
LDTF	Lineage-determining transcription factors
LPM	Large peritoneal macrophage
LPS	Lipopolysaccharides
M-CSF	Macrophage colony-stimulating factor
mTOR	*Mammalian target of rapamycin*
NF-κB	Nuclear factor kappa-light-chain-enhancer of activated B cells
NLRP3	NOD-like receptor family, pyrin domain containing 3
NOD2	Nucleotide-binding oligomerization domain-containing protein 2
NR	Nuclear receptor
P	Postnatal day
P-adj	Adjusted p value
PBS	Phosphate buffered saline
PCA	Principal component analysis
PPAR-γ	Peroxisome proliferator activated receptor gamma
PAP	Pulmonary alveolar proteinosis
Pre-AM	Pre-alveolar macrophage
RNA-seq	RNA sequencing

RUNX   Runt-related transcription factor

SD   Standard deviation

SDTF   Signal-dependent transcription factor

SMAD   SMAD family member

Sn   Sialoadhesin

STAT   Signal transducer and activator of transcription

TF   Transcription factor

TGF-β Transforming growth factor beta

TNF   Tumor necrosis factor

TLR   Toll like receptor

TSS   Transcription start site

VHL   Von Hippel-Lindau tumor suppressor protein

LIST OF FIGURES AND TABLES

ACKNOWLEDGEMENTS

First, I would like to recognize the UCSD Biomedical Sciences Program for providing a supportive environment to pursue training and research of my interest. I would also like to thank my thesis committee members, Dr. Chris Glass, Dr. Yury Miller, Dr. Stephen Spector, and Dr. David Traver. Thank you to my mentor, Dr. Lawrence Prince, for your support, guidance, and encouragement throughout this journey. Finally, I would like to acknowledge the National Institute of Health for financing my graduate training.

I would like to extend my gratitude to all of those whom I have had the pleasure to work with. Our collaboration with the Glass lab was invaluable. Thank you Marten and Mashito for your guidance and sharing your knowledge and excitement for science. I am also grateful for my colleagues in Prince and Hoffman lab especially Erika, Sean, Omar, Alyssa, Lori, and Laela. Thank you for your discussions, advice, and friendship. I very much value our time together.

I would like to thank my past mentors Dr. Yokobayashi, Yoko, Vandy, Naoya, and J Tso for sparking my interest in science and providing an exciting environment and ample resources for me to pursue the research career that I have always wanted.

To my family and grandparents in Japan, I am grateful for your warmth and endless support. Thank you, Yuzu and Kaito for the strength you have given me. And most of all to my husband Tomoya, thank you always for thinking what is best for me.

This dissertation contains material currently in preparation for submission. The dissertation author is the primary investigator.

VITA

2010   Bachelor of Science, University of California Davis

2020   Doctor of Philosophy, University of California San Diego

PUBLICATIONS

1. Lund, S. J., Patras, K. A., Kimmey, J. M., **Yamamura, A.**, Butcher, L. D., Del Rosario, P. G., ... & Prince, L. S. (2020). Developmental Immaturity of Siglec Receptor Expression on Neonatal Alveolar Macrophages Predisposes to Severe Group B Streptococcal Infection. *Iscience*, *23*(6), 101207.

2. Lakhdari, O., **Yamamura, A.**, Hernandez, G. E., Anderson, K. K., Lund, S. J., Oppong-Nonterah, G. O., ... & Prince, L. S. (2019). Differential Immune Activation in Fetal Macrophage Populations. *Scientific reports*, *9*(1), 1-13.

3. Oppong-Nonterah, G. O., Lakhdari, O., **Yamamura, A.**, Hoffman, H. M., & Prince, L. S. (2019). TLR Activation Alters Bone Marrow-Derived Macrophage Differentiation. *Journal of innate immunity*, *11*(1), 99-108.

4. Yuan, X., Yang, B. H., Dong, Y., **Yamamura, A.**, & Fu, W. (2017). CRIg, a tissue-resident macrophage specific immune checkpoint molecule, promotes immunological tolerance in NOD mice, via a dual role in effector and regulatory T cells. *Elife*, *6*, e29540.

5. Sharma, V., **Yamamura, A.**, & Yokobayashi, Y. (2012). Engineering artificial small RNAs for conditional gene silencing in Escherichia coli. *ACS synthetic biology*, *1*(1), 6-13.
6. Nomura, Y., Sharma, V., **Yamamura, A.**, & Yokobayashi, Y. (2011). Selection of silk-binding peptides by phage display. *Biotechnology letters*, *33*(5), 1069-1073.

ABSTRACT OF THE DISSERTATION

Role of the Lung Microenvironment in Regulating Adult and Neonatal AM Transcriptional
Activity

by

Asami Yamamura

Doctor of Philosophy in Biomedical Sciences

University of California San Diego, 2020

Professor Lawrence Prince, Chair

Alveolar macrophages (AMs) play critical roles in metabolizing surfactant and
protecting the lung against inhaled pathogens. AMs mature following the newborn period and
their immaturity at birth may contribute to the variety of infectious and inflammatory lung
diseases specifically affecting infants. However, the specific molecular features differentiating
neonatal and adult AMs remain poorly understood. Here we identify the unique transcriptomes
and enhancer landscapes of neonatal and adult AMs that establish the molecular phenotypes
specific to each developmental age. Adult AMs expressed higher levels of genes involved in

lipid transport and metabolism (i.e. *Fabp1, Pnpla5*), consistent with their role in surfactant recycling. Neonatal AMs expressed higher levels of proinflammatory genes (*Il1b, Il6, Tnf, and S100a8*). ATAC-seq data detected adult AM peaks enriched with motifs recognizing KLF, GR, PPAR-γ, and STAT. Accessible chromatin regions in neonatal AMs were highly enriched with binding motifs for the innate immunity transcription factors AP1, NF-κB, and IRF. To test how these baseline differences might impact AM innate immune function, we exposed neonatal and adult mice *in vivo* with inhaled LPS. AMs from both neonatal and adult mice demonstrated robust induction of Toll-Like Receptor 4 (TLR4) signaling pathways and similar patterns of chromatin accessibility. While neonatal and adult AMs did exhibit divergent expression patterns for some genes, the overall core innate response was similar. Intriguingly, neonatal AMs expressed higher basal levels of many LPS-induced genes, suggesting constitutive innate immune priming or activation in the neonatal lung. The lung microenvironment was a major factor regulating the unique molecular features of neonatal and adult AMs. Culturing isolated AMs for only 20h minimized the differences in gene expression between neonatal and adult cells. Interesting, while neonatal AMs in culture more closely resembled adult AMs, a core inflammatory signature of gene expression was retained. These data suggest that the proinflammatory phenotype of neonatal AMs results from both inherent properties of the cell and the lung microenvironment. Collectively, these studies provide new insights into the molecular mechanisms of lung innate immune development.

INTRODUCTION

Newborns and Inflammatory Lung Disease

During the first month of life, newborns are highly vulnerable to lung infection and inflammation (1-3). Pneumonia remains a leading cause of newborn death in the U.S. and worldwide, accounting for almost 10% of childhood mortality (4). Based on the time of manifestation, neonatal pneumonia can be classified as either early-onset (within 7 days of life) or late-onset disease (occurs after 7 days). In most cases of early-onset pneumonia, bacterial pathogens are passed from infected amnionic fluid or maternal genital tract during delivery. Group B *Streptococcus* (GBS) followed by gram-negative bacteria *Escherichia coli* (*E. coli*) are the most common causes of perinatal pneumonia. Late-onset pneumonia, in contrast, generally are community-acquired and transmitted to the hospitalized infants after birth from infected individuals or contaminated equipment (5). Of note, birth weight and prematurity is associated with increased risk for pneumonia and the morality rate is higher in early onset compared to late onset (6, 7). Intriguingly, many of the neonatal pathogens rarely cause serious infections in healthy older children and adults.

Lung inflammation also plays a role in the pathogenesis of bronchopulmonary dysplasia (BPD), a chronic developmental lung disease affecting up to 50% of infants born before 28 week gestation (8-12). In response to infection, hyperoxia, and mechanical ventilation, pulmonary inflammation disrupts normal lung development, resulting in arrested airway branching and fewer alveolar units (8, 13-15). Clinically, increased risk of BPD is associated with increase in pro-inflammatory cytokines. Tracheal aspirates from infants with BPD exhibit enhanced expression levels of tumor necrosis factor alpha (TNFα), interleukin 8 (IL-8), IL-6, and IL-1β (16-18). Consistently, experimental mouse model for BPD demonstrated in utero

1

exposure to bacterial endotoxin reduces airway morphogenesis and inhibits the expression of key growth factors for lung development (19). Patients with BPD experience long-term health consequences of frequent hospitalization and persistent abnormalities of lung function (20, 21).

Why the newborn period represent a window of high susceptibility to inflammatory lung disease remain poorly understood. Our laboratories studies the mechanisms linking neonatal immunity and lung inflammation. We focus on understanding the development of lung immunity, specifically the macrophages, and their contributions to disease process within the developing lung.

Role of Macrophages in Newborn Lung Disease

Macrophages are the primary phagocytic cells of the innate immune system and orchestrate the process of inflammation, including its initiation, progression, and resolution. In the lung, macrophages ingest inhaled pathogens and regulate surfactant homeostasis (22-25). However, dysregulation of lung macrophage functions contributes to the pathogenesis of multiple diseases, including diseases in the neonatal period.

In preterm infants, macrophage activation is linked to inflammation and defective lung morphogenesis, causing BPD (26-28). Mechanistic studies from our laboratory and others have provided evidence that inflammatory stimuli inhibit the expression of multiple genes essential for branching morphogenesis; bacterial endotoxin, NF-κB activation, and NLRP3 inflammasome activation, each induces inflammation and disrupts normal lung development. Using a novel NF-κB transgenic reporter mouse, we identified macrophages as the primary cellular sites of inflammation (26). Subsequent studies further demonstrated IL-1β released from the macrophages as the key inflammatory mediator causing abnormal lung phenotype

(27). Collectively, these studies show macrophage activation and inflammatory cytokine release as key mechanisms contributing to BPD.

In newborns, developmental immaturity of lung macrophages at birth predisposes to severe GBS infection (29). Our novel murine model of newborn GBS pneumonia recapitulate important features of human disease. Following infection, neonatal mice exhibit accumulation of GBS in the lung, persistent lung injury, and enhanced mortality rate compared to older mice. Using this model, we found macrophages from neonatal mice are unable to effectively phagocytose and kill GBS, leading to lung injury and bacteremia. We further showed that compared to adult macrophages, newborn macrophages express significantly reduced level of cell surface Siglec receptor Sialoadhesin (Sn) for effective detection and killing of GBS (29). Our findings demonstrate that newborn macrophages lack the fully differentiated phenotype and function present in adults, consequently rendering the newborn vulnerable to disease.

Dynamic changes in the expression of many genes critical for the macrophage inflammatory response in the postnatal lung also suggests developmental program of macrophages (27). Expression of proinflammatory genes such as *Il1b*, *Aim2*, *Nlrp3*, and *Nod2* are highly expressed in newborn compared to adult (27). Collectively, these data provide a compelling incentive to identify unique molecular features of neonatal macrophages.

Lung Development and Transition at Birth

At birth, the neonatal lung is still undergoing development. This period of lung development also coincides with a period of when newborns are most sensitive to infection and inflammation. Lung development comprises of five distinct stages in mice, occurring both pre- and postnatally. Embryonic phase of lung development begins on gestation day 9 (E9) in mice,

involving the formation of the trachea and two primary lung buds. During the pseudoglandular stage, from E12 to E16, branching morphogenesis drive the formation of airways and tree-like structures (30). Beginning at E16 in the canalicular stage, distal airways form and vascularization and angiogenesis occur, increasing lung size. The saccular stage begins at E17 and continues into postnatal day 5 (P5). During this stage, the distal ends of branches form alveoli and thinning of the interstitium begins. The final stage of lung development is the alveolar stage. From P5 to P30, the saccules undergo further subdivision into mature alveoli and increases the overall surface area for efficient gas exchange (31).

The transition at birth from a largely protective environment in the womb to an extra-uterine world represents the most complex adjustment period for the newborn lung (32). Cellular composition and organization changes drastically during this critical transition. Epithelial precursors differentiate into type 1 and type 2 alveolar cells. Type1 cells facilitate gas exchange between alveoli and blood vessels while, type 2 cells secrete surfactant to prevent atelectasis (25, 33). Apoptosis and differentiation of mesenchymal cells lead to thinning of the interstitium, supporting gas exchange (31, 34, 35). Diverse immune cells migrate into the lung, providing front line defense against immunological challenges (36). Simultaneously, the neonatal lung experiences a drastic environmental shift with clearance of amniotic and fetal lung fluid, surfactant secretion, and the onset of breathing (37). The transition is also coupled with exposure to commensal microbiota as well as harmful microbial pathogens (38-40). Together, the incomplete lung development and environmental transition represents a fragile window in which newborns fall short to meet diverse immunological demands and are vulnerable to tissue damage, succumbing to inflammatory diseases.

Development of Lung Macrophages

The fetal immune system development occurs in parallel with the ongoing lung development. Prior to the development of bone marrow, earliest embryonic hematopoiesis occurs in the yolk-sac blood islands at E7. Multiple myeloid populations seed the embryonic and fetal tissues in successive waves (41-43). Primitive macrophages arise from erythromyeloid precursors in the yolk-sac blood islands during primitive hematopoiesis. Upon the establishment of the circulatory system from E8 to E10, these macrophage populations spread into embryonic tissues. Concurrently, definitive hematopoiesis occurs in the aorta-gonads-mesonephros (AGM) and generate all hematopoietic lineages, including the progenitors that colonize the fetal liver. These progenitors differentiate into fetal monocytes in the fetal liver and populate the peripheral organs at around E14. As definitive hematopoiesis moves the sites to the bone marrow (BM), circulating monocytes gradually dilute the embryonic-derive macrophage populations (41-43). Most tissue resident macrophage arise from fetal monocyte populations, with an exception of microglia which are derived yolk-sac derived macrophages (44).

The waves of myeloid cells recruited to the lung during development can be clearly identified. At E12, the fetal lung contains F4/80^{hi} CD11b^{lo} macrophages which most resemble the phenotype of macrophages from the yolk sac. At E14, F4/80^{lo} CD11b^{hi} cells begin to migrate from the fetal liver to the fetal lung. While the number of yolk-sac macrophage remains unchanged between E17 and a week after birth, fetal monocyte population proliferate dramatically and differentiate into pre-alveolar macrophage (pre-AM) and eventually into AMs. During the differentiation, fetal monocytes successively acquire their expression of CD11c, Siglec-F, and F4/80 and lose their expression of Ly6C and CD11b to give rise to AMs (36, 45,

46). Like many other tissue macrophages, AMs self-maintain through local proliferation into and throughout adulthood, independently of BM-derived cell contribution (36, 47). Although fetal monocytes are the primary source of mature AMs, yolk-sac macrophage and adult bone-marrow monocytes are all capable of seeding the alveolar niche and differentiating into mature AMs. These observations suggest the instructive role of the local tissue signals in driving AM development (44).

Regulators of Alveolar Macrophage Development

Despite sharing common embryonic progenitors, tissue macrophages acquire distinct identity and functions specific to their tissue of residence. Accordingly, each tissue macrophage exhibits a unique transcriptional profile. Multiple evidence supports the role of environmental factors in shaping the specialized identity of tissue macrophages (48-50). AMs derived from adoptive transfer of bone marrow monocytes or peritoneal macrophages into the lung microenvironment acquire a gene expression profile strikingly similar to that of endogenous embryonically derived AMs (48, 51). Conversely, transfer of microglia (resident embryonic derived brain macrophages) or peritoneal macrophages from their tissue niche into the culture environment rapidly alters the expression of their unique gene signatures (50, 52).

Multiple tissue derived factors have been shown to regulate AM maturation and function, including granulocyte-macrophage colony-stimulating factor (GM-CSF) and transforming growth factor-β (TGF-β). GM-CSF is a major growth factor and immune modulator produced by epithelial cells, crucial for the perinatal development of AM (36, 45). Exposure to GM-CSF induces expression of the nuclear receptor PPAR-γ in fetal monocytes, which in turn confers AM signatures (45). AM development is also dependent on cell-

autonomous TGF-β signaling. In concert with GM-CSF, TGF-β promote the expression of PPAR-γ (46). Loss of GM-CSF, TGF-β, or PPAR-γ expression in mice results in defective AM differentiation and function which contributes to the development of pulmonary alveolar proteinosis (PAP), a disease characterized by the accumulation of surfactant in the alveoli (36, 45, 46).

The role of oxygen sensing on AM maturation adds a layer of complexity to the environment cues guiding AM development. The emergence of AM from Pre-AM coincides with a drastic increase in oxygen concentration, as the lung environment transitions from hypoxia to normoxia following birth. Von Hippel-Lindau tumor suppressor protein (VHL) is a negative regulator of hypoxia-inducible factors (HIFs), the master transcription factor (TFs) of the cellular response to low oxygen tension. AMs deficient in VHL are desensitized to increasing oxygen concentration in the postnatal lung. VHL deletion in AMs results in immature AM phenotype, altered metabolic profile, and defective capacity to remove surfactant (53, 54).

It is unlikely that aforementioned tissue signals are the sole drivers of the AM differentiation. Additional factors including, Bach2, STAT5, C/EBPβ, and mammalian target of rapamycin (mTOR) are also implicated in the imprinting of AM identity and function. AMs from mice deficient in each of these factors exhibit immature phenotype and develop PAP (55-58). If and how these molecular signals interact to establish AM identity remain to be investigated. In addition, it would be of substantial interest to better understand the sources of the tissue signals and the developmental time point in which these signals induce AM signature profiles.

Enhancer Landscapes of Tissue-resident Macrophages

Investigation of molecular mechanisms responsible for tissue-specific programs of macrophages revealed that each macrophage population expresses distinct combination of TFs and exhibits distinct epigenomic signatures. Both ontogeny and environmental signals are integrated at the genomic level to drive distinct transcriptional programs of tissue macrophages (48, 50). Epigenetic modification, specifically the chromatin accessibility, plays a critical role in regulating gene expression. Open chromatin regions, devoid of nucleosomes, contain enhancers and promoters, collectively known as regulatory elements (59). In contrast to promoters, enhancers exhibit enrichment for motifs that recognize lineage-determining transcription factors (LDTFs) that bestow cell-type specificity (48, 50). In macrophages, PU.1 acts as the key LDTF that initiates chromatin accessibility and enhancer selection. Cooperative interactions between PU.1 and additional LDTFs, including C/EBP, AP-1, IRF and RUNX, are required to establish macrophage-specific enhancer landscape (60).

Cell-type specific responses to external signals are achieved through the action of signal-dependent transcription factors (SDTFs). Examples of SDTFs include NF-κB, nuclear receptors, and STAT factors (60-62). The open chromatin regions established by LDTFs serve as major sites for the binding of SDTFs (63-66). Genome-wide mutagenesis studies using natural genetic variation have indicated the collaborative and hierarchical interactions between LDTFs and SDTFs at pre-established enhancers (64). Mutations in PU.1 binding motifs abolish the binding of C/EBPα. Similarly, mutations in C/EBPα binding result in the loss of cooperative binding of PU.1. While the mutations in either LDTF motifs abolish NF-κB binding, the NF-κB motif mutations rarely influence the binding of LDTFs. Additionally, in response to certain stimuli, SDTFs could directly bind to inaccessible regions of chromatin to

establish "latent" or "de novo" enhancers in collaboration with LDTFs (61, 63, 65). Following macrophage activation using TLR4 ligation, for example, the p65 subunit of NF-κB binding occurs primarily at pre-established enhancers but also occurs at de novo enhancers in concert with PU.1 and C/EBPα.

Genomic analysis of macrophages isolated from distinct tissues indicated that each population expresses a unique combination of TFs and exhibits tissue-specific enhancer repertoires (48, 52). A comparison of enhancer regions between large peritoneal macrophage (LPM) and microglia, for example, revealed that around 20% of the enhancers are restricted to each population and these enhancers are in the vicinity of differentially expressed genes (50). Motif enrichment analysis of enhancer regions specific to microglia and LPM identified motifs assigned to GATA and SMAD, respectively. Evidence suggests signals from the environment induce the expression of unique TFs, which in turn shape tissue-specific enhancer repertoires. In the peritoneum, for example, retinoic acid is the tissue derived signal which induce GATA-6 in LPM (50, 52). Together, these studies emphasize the crucial roles of local environmental signals in regulating distinct sets of TFs that select and activate tissue-specific enhancers to imprint specialized macrophage phenotypes.

Research Plan Description

AMs in the lung perform specialized functions ranging from maintenance of surfactant homeostasis to protection against inhaled microbes. In mice, AMs arise from fetal myeloid precursors within the first week following birth. This perinatal transition coincides with a unique window of vulnerability to lung infection and injury, suggesting immaturity of AM function. Dysregulation of macrophage immune functions within the developing lung

contributes to severe pathology in mouse models of BPD and pneumonia (26, 27, 29), diseases specifically affecting newborns. Expression of many genes critical for the macrophage inflammatory response are developmentally regulated, with the highest expression around birth (27). While AMs are clearly one of the major cells mediating lung immunity, their molecular and functional changes during postnatal lung development remain largely unknown. In the present study, we evaluated transcriptional profiles and open chromatin regions of neonatal and adult AMs to understand the differences in the molecular features that may exist between these cells. Integration of these data identified distinct sets of TFs that shape the enhancer repertoires and phenotypes specific to each developmental age. To examine how these baseline differences contribute to AM innate immune response, we stimulated neonatal and adult mice with LPS intranasally. Furthermore, we provide evidence for the instructive role of the lung microenvironment in regulating distinct phenotypes. Transferring AMs to a tissue culture environment resulted in rapid loss of unique transcriptional signatures and enhancer landscapes. Together, these findings provide insights into the regulatory mechanisms of AM identify and functions during lung development.

Mice

The Institutional Animal Care and Use Committees from the University of California at San Diego approved all animal experiments. C57BL/6 mice were obtained from Envigo and bred in house. Both sexes were used for experiments up to 2 weeks of age. Male mice were used at between 2 to 10 weeks of age.

Intranasal Instillation of LPS

Mice were anesthetized with isoflurane (MWI Veterinary Supply) before intranasal (i.n.) instillation of LPS (*Escherichia coli* O55:B5; Sigma-Aldrich). Neonatal (postnatal day 4) and adult (8 to 10 weeks of age) mice were challenged with 5ul or 50ul of LPS diluted in sterile saline, respectively, at 0.1ug/g body weight. The control mice received sterile saline. All mice were sacrificed 2 h after intranasal delivery of LPS.

Preparation of Cells

Neonatal mice up to 7 days of age were sacrificed by decapitation and mice older than 7 days of age were euthanized by CO_2 inhalation. Lungs were perfused intracardially through the right ventricle with cold PBS. Lung tissue was minced and enzymatically digested in RPMI-1640 (Corning 10-040-CV) containing 50 U/ml DNase I (Roche 10104159001), 400 ug/ml Liberase TM (Roche 5401119001), and Flavoperidol (1uM, Sigma Aldrich) at 37 ˚C for 15 min. Tissue homogenates were passed through a 100 um cell strainer (Fisher Scientific) and erythrocytes were lysed with ACK buffer (Life Technologies). Prior to antibody staining, the cell suspensions were filtered through a 70 um cell strainer (Fisher Scientific).

Flow Cytometry and Cell Sorting

Single cell suspensions were resuspended in PBS with CD16/CD32 blocking antibody (Biolegend) and Zombie Aqua (Biolegend) for 20 min. The cells were then incubated with fluorochrome-conjugated antibodies in staining buffer (HBSS containing 2% FBS and 2mM EDTA) for 1h. For intracellular staining, cells were fixed and permeabilized using a Foxp3 staining buffer set as described in the manufacturer's protocol (eBiosciences). The following antibodies were used for cell sorting and analysis: CD45.2 (Biolegend, clone 104), F4/80 (Biolegend, clone BM8), CD64 (BD Biosciences, clone X54-5/7.1), Siglec-F (BD Biosciences, clone E50-2440), CD11b (Biolegend, clone M1/70), CD11c (Biolegend, clone N418), Ly-6G (Biolegend, clone 1A8), Ly-6C (BD Biosciences, clone AL-21), I-A/I-E (Biolegend, clone M5/114.15.2), and pro-IL1β (Thermo Fisher, clone NJTEN3). Samples were acquired and assessed on a BD FACSCanto II or BD FACSAria II (BD Biosciences) and analyzed with FlowJo software (FlowJo, LLC). Sorting was performed on a BD FACSAria II. Lung macrophage subsets were identified using the following gating strategy: Doublets were excluded using side scatter height (SSC-H) vs side scatter width (SSC-W), followed by forward scatter height (FSC-H) vs forward scatter width (FSC-W). Viable cells were selected using Zombie Aqua LIVE/DEAD stain. Immune cells were identified as $CD45^+$ cells and neutrophils were outgated using Ly-6G. Macrophages were defined as CD64 and F4/80 double-positive cells and was further divided into Siglec-F^+ $CD11b^-$ AMs and Siglec-F^- $CD11b^+$ IMs.

Primary Culture of Lung Macrophages

Freshly isolated lung macrophages were plated in 96-well plates at 60,000 to 100,000 cells. Culture media consisted of RPMI-1640, supplemented with 10% FBS, 100 U/mL

penicillin/streptomycin, and 4 ng/mL rmM-CSF (R&D, 416-ML010). For experiments examining the effects of tissue culture environment on macrophage gene expression, cells were harvested between 0 h to 20 h of tissue culture. For studies investigating the effects of LPS on immune response of macrophages in culture, cells were stimulated with 250 ng/mL LPS (*Escherichia coli* O55:B5; Sigma-Aldrich) for 2 h either immediate after isolation or after 10 h and 20 h of tissue culture. Cells were washed with cold PBS, and then either lysed in 300 ul of TRIzol reagent (Thermo Fisher; see below) for RNA-Seq or in 50 ul lysis buffer (10 mM Tris-HCl pH7.5, 10mM NaCl, 3mM MgCl2, 0.1% IGEPAL CA-630; see below) for ATAC-Seq.

Quantitative Real-time PCR

Sorted lung macrophages were in lysed and homogenized in TRIzol reagent (Thermo Fisher) and total RNA was purified with Direct-zol RNA Miniprep (Zymo Research). cDNA was synthesized using SuperScript IV VILO master mix (Invitrogen). qPCR was performed using iQ SYBR Green supermix (Bio-Rad) on a CFX96 Touch Real-Time PCR Detection System (Bio-Rad). Gene expression levels were represented using 2^{-ddCt} method and normalized to the reference gene *GAPDH*. The following primers were used: *GAPDH* Fw: 5'-AGT ATG ACT CCA CTC ACG GC-3' and *GAPDH* Rv: 5'-CAC CAG TAG ACT CCA CGA CA-3'; *Il1b* Fw: 5'-GAC CTG TTC TTT GAA GTT GAC GGA CC-3' and *Il1b* Rv: 5'-CAA TGA GTG ATA CTG CCT GCC TGA AG-3'; *Il6* Fw: 5'-AAA CCG CTA TGA AGT TCC TCT CTG-3' and *Il6* Rv: 5'-ATC CTC TGT GAA GTC TCC TCT CC-3'; *Tnfa* Fw: 5'-ATG AGC ACA GAA AGC ATG ATC-3' and *Tnfa* Rv: 5'-TAC AGG CTT GTC ACT CGA ATT-3'.

RNA Sequencing

Purified total RNA was assessed for quality using an Agilent Tapestation 4200. Samples with an RNA Integrity Number (RIN) of at least 8.0 or greater were used to generate RNA sequencing libraries using the TruSeq Stranded mRNA Sample Prep Kit with TruSeq Unique Dual Indexes (Illumina, San Diego, CA). 60 ng of total RNA from each sample was processed following manufacturer's specifications, adjusting RNA shear time to five minutes. Resulting RNA libraries were multiplexed and sequenced with 75 base pair (bp) single reads (SR75) to a depth of approximately 25 million reads per sample on an Illumina HiSeq 4000. Samples were demuxltiplexed using bcl2fastq v2.20 Conversion Software (Illumina, San Diego, CA).

ATAC Sequencing

25,000 sorted AMs were lysed in 25 ul lysis buffer (10 mM Tris-HCl pH7.5, 10mM NaCl, 3mM MgCl2, 0.1% IGEPAL CA-630). 1.25 ul Tagment DNA enzyme I (Illumina 15027865) was added and incubated at 37°C for 30 min. DNA was extracted with the Zymogen ChIP DNA purification kit (Zymo) and then amplified using the Nextera Primer Ad1, Nextera Barcode Primers Ad2.n, SYBR Green, and NEBNext High-Fidelity 2X PCR Master Mix for 5-15 cycles. PCR reactions were size selected for 160-280 bp by gel extraction (10% TBE gels, Life Technologies EC62752BOX) and then 75 bp single-end sequenced for 51 cycles on a HiSeq 4000.

Data Analysis

RNA Sequencing Analysis

Quality control of the raw fastq files was performed using the software tool FastQC (67) v0.11.3. Sequencing reads were trimmed with Trimmomatic (68) v0.36 and aligned to the mouse genome (GRCm38.p6 (71) using the STAR aligner (69) v2.5.3a. Read quantification was performed with RSEM (70) v1.3.0 and the Gencode release vM19 annotation (71). The R BioConductor packages edgeR7 and limma8 were used to implement the limma-voom9 method for differential expression analysis. In brief, lowly expressed genes—those not having counts per million (cpm) ≥ 3 in at least 3 of the samples—were filtered out and then trimmed mean of M-values (TMM) (72) normalization was applied. The experimental design was modeled upon condition (~ 0 + condition). The voom method was employed to model the mean-variance relationship in the log-cpm values weighted for inter-subject correlations in repeated measures of patients, after which lmFit was used to fit per-gene linear models and empirical Bayes moderation was applied with the eBayes function. Significance was defined by using an adjusted p-value cut-off of 0.05 after multiple testing correction (73) using a moderated t-statistic in limma. Functional enrichment of the differentially expressed genes was performed using WebGestalt (74) (including GSEA (75)), GSVA (76) and SPIA (77).

ATAC Sequencing Analysis

ATAC samples were mapped to the mm10 genome using Bowtie2 (78). IDR (79) peak files were generated for each condition. Pair-wised comparisons using DESeq2 (80) were performed for all groups and specific peak subsets ($Log_2FC > 1$, p-adj < 0.05) were selected for further analysis. For the de-differentiation experiments, only peaks that were close to downregulated

genes were selected. Motif analysis was performed using a specific or random background using HOMER (60) on peaks that were significantly different compared to the other condition. ATAC-seq data was visualized using the UCSC genome browser (81).

RESULTS

Unique Transcriptional Signatures Differentiate Adult and Neonatal AMs

To identify the molecular differences between adult and newborn AMs, we compared gene expression in C57BL/6 mice at postnatal day 4 (P4) and 8-10 wk of age. As AMs mediate the initial immune response to microbial challenge in the lung, both adult and neonatal mice were challenged with intranasal LPS to measure potential developmental differences in the innate immune response. Control mice received sterile, endotoxin free PBS. After 2 h, we isolated Siglec-F$^+$ CD11b^{lo} AMs by fluorescence-activated cell sorting (FACS) (Figure 1A). Importantly, P4 represents the first day during mouse development that that cell surface markers clearly distinguish AM populations in the newborn lung. RNA-seq was performed to identify transcriptional differences between newborn and adult cells. Principal component analysis (PCA) showed that replicate samples from neonatal and adult AMs grouped together based on their transcriptional profiles (Figure S1A).

We first analyzed cells from PBS treated control mice to compare differences between adult and neonatal AMs at baseline. RNA-seq analysis revealed neonatal AMs contained a higher number of differentially expressed genes (1481) compared to adults (651) (fold change [Log$_2$FC] > 1, adjusted p [p-adj] < 0.05) (Figure 1B). Expression of AM signature genes (82) was largely similar between adult and neonatal AMs (63 of 108 signature genes with similar expression) (Figure 1C). Expression of known AM genes *Cebpb, Car4,* and *Atf5* are shown in Figure 1D. The differential expression of 45 AM signature transcripts in adult cells compared to neonates likely represents ongoing AM maturation at P4. Neonatal AMs expressed higher levels of classical monocyte signature genes, consistent with their differentiation from fetal monocyte precursors (Figure 1D). Therefore, while the neonatal lung at P4 is populated by cells

17

largely acquiring the AM transcriptional program, differentiation into mature AMs appeared incomplete.

We next interrogated the entire list of differentially expressed genes in adult and neonatal AMs using Metascape. Adult AMs expressed higher levels of genes playing roles in solute and molecular transport and fatty acid metabolism, consistent with the lipid-rich alveolar microenvironment and the role of AMs in surfactant homeostasis. Neonatal AMs were enriched in transcripts involved in vascular development, morphogenesis, and immunity (Figure 1E). Figure 1F illustrates higher expression of *Pparg, Fabp1, Pnpla5, Mtss1,* and *Slc9a4* in adult AMs compared to neonatal AMs along with elevated expression of *Il1b*, *Tnf*, *S100a84*, *Pdgfb* and *Mmp12* in neonatal AMs. Ingenuity pathway analysis (IPA) revealed genes enriched in adult AMs were associated with LXR/RXR activation and PPAR signaling while neonatal AMs were enriched for genes related to Toll-like receptor signaling and NF-κB activation (Figure S1B). These analyses suggest a pro-inflammatory phenotype in neonatal AMs when compared to adult cells. To better characterize the expression dynamics of these inflammatory transcripts, we measured *Il1b* expression in lung macrophage populations during fetal development and into adulthood (Figure S1C). Expression of *Il1b* increased during late gestation and peaked on the day of birth before falling in differentiated AMs over time. Collectively, these data demonstrate that upon differentiation into AMs, neonatal lung macrophages possess a very distinct transcriptional profile related to tissue morphogenesis and activation of the innate immune response.

Distinct Transcriptional Regulators Inferred from Open Chromatin Profiles

To gain insights into potential epigenetic mechanisms underlying the differential transcriptional programs of adult and neonatal AMs, we identified open chromatin regions using an assay for transposase-accessible chromatin (ATAC-seq). The ATAC-seq tracks illustrated in Figure 2A highlight examples of chromatin regions that are similarly and differentially accessible. We found genes critical for macrophage and AM lineage determination and differentiation, such as *Spi1* and *Pparg*, exhibited similar open chromatin profiles at putative regulatory elements in neonatal and adult AMs. In contrast, chromatin regions adjacent to *Fabp1* and *Chil3*, were more accessible in adult AMs. Upregulation of macrophage marker *Chil3* (encoding Ym1) has been previously described with AM differentiation and alternatively activated macrophage populations (83). Neonatal AMs contained more open chromatin regions neighboring the TGF-β signaling component *Smad3* and the platet-derived growth factor member *Pdgfb*. Of note, TGF-β is required for maturation of AMs in the neonatal lung (46).

Genome-wide comparison of ATAC-seq peak tag counts indicated only a modest number of genomic sites with differentially open chromatin between adult and neonatal AMs. While 88 peaks were enriched in adult AMs, 66 peaks were enriched neonatal AMs (Figure 2B). The low number of unique peaks suggested relatively similar chromatin environment. Restricting our analysis to known motifs, motifs recognizing myeloid lineage TF, PU.1 were significantly overrepresented in both neonates and adults. However, known motif and de novo enrichment analysis of ATAC-seq peaks (>2kb from a transcription start site (TSS)) also returned motifs assigned to distinct TFs in adult and neonatal AMs (Figure 2C, S1D). Analysis of accessible chromatin regions enriched in adult AMs identified predicted

motifs for KLF, GR (Nuclear Receptor), and STAT (Figure 2C). Neonatal-enriched regions exhibited significant overrepresentation of IRF, AP-1, and NF-κB, consistent with the inflammatory gene expression profiles observed by RNA-seq (Figure 1E, 1F, and 2C). These data show that neonatal AMs have additional chromatin accessibility to stimulus-dependent TF binding sites, potentially leading to differential transcriptional profiles and basal inflammatory activation.

We next compared the expression levels of TF family members whose motifs were identified by ATAC-seq, focusing primarily on TF with expression above 16 CPM and with differential expression between adult and neonatal AMs. In both adult and neonatal AMs, *Spi1* (encoding the canonical macrophage TF PU.1) showed the highest expression among the ETS domain TF family (Figure S1E). Of the KLF family, adult AMs expressed high levels of *Klf4*, which is rapidly upregulated as AM precursors enter the developing lung (Figure 2D) (84). Adult AMs also expressed high levels of *Nr3c1* and *Pparg,* predicted to bind NR sites and implicated in AM maturation. While *Stat1*, *Stat3*, and *Stat6* were most abundant, *Stat2*, *Stat5a*, and *Stat5b* were more highly expressed in adult AMs (Figure 2D). Neonatal AMs expressed higher levels of multiple IRF, AP-1, and NF-κB family members compared to adult AMs (Figure 2E), with highest expression of *Irf5* and the AP-1 family members *Junb*, *Fosl2*, and *Atf4*. NF-κB family members *Nfkb1*, *Nfkb2*, *Relb*, and *Rel* were all upregulated in neonatal AMs (Figure 2E). Together, these data characterize the distinct profiles regulating AM transcription in the adult and neonatal lung, involving both TF expression and changes in the promoter/enhancer landscape.

LPS Induces Robust Innate Immune Response in Adult and Neonatal AMs In Vivo

Data from control AMs clearly demonstrated a more pro-inflammatory phenotype in neonatal AMs. However this pattern of gene transcription represented baseline conditions and did not address the response to microbial challenge. We therefore compared the response of adult and neonatal AMs to LPS challenge to test for potential differences in the innate immune response. LPS induced robust recruitment of neutrophils and monocytes into adult lungs, consistent with acute lung inflammatory response. In contrast, frequency of AMs was reduced following LPS exposure. In the neonatal lungs, we observed similar trends but with moderate changes in the neutrophil migration and AM reduction (Figure S2A). In the lung, both AMs and Siglec-F$^-$ macrophages (IM) respond to inflammatory stimuli. After intranasal LPS treatment, we measured pro-IL-1β expression in both cell populations. As seen in (Figure S2B), AMs from neonates expressed baseline levels of pro-IL-1β. The percentage of pro-IL-1β-positive AMs was similar in neonates and adults. A smaller percentage of IM also expressed IL-1β after LPS exposure, with again similar response between adults and neonates (Figure S2C). These results identified AMs as the major cellular site of innate immune activation in both adult and neonatal lungs.

RNA-seq analysis on isolated AMs following LPS exposure identified twice as many differentially expressed genes in adults (2207) compared to neonates (950) (Log$_2$FC > 1, p-adj < 0.05) (Figure 3A). Similarly, we observed a dramatically higher number of downregulated genes in adult AMs. In both adults and neonates, IPA functional analysis of differentially expressed genes following in vivo LPS treatment included the major pathways downstream of the LPS receptor TLR4 (toll-like receptor signaling, NF-κB signaling, and p38 MAPK signaling, Figure 3B). However LPS activation of adult AMs also led to upregulation of genes

associated with interferon signaling. Metascape analysis performed on upregulated genes yielded similar results as the IPA analysis, with enrichment for pathways related to inflammatory response in both adult and neonatal cells (Figure S2D).

At first glance, the increased number of LPS-activated transcripts in adult AM might suggest a more robust innate immune response in adults compared to neonates. However, we detected enrichment in transcripts involved in inflammation and TLR4 signaling pathways in neonates in control samples (Figure 3B). Consistently, identifying LPS-activated genes ($\text{Log}_2\text{FC} > 2$, p-adj < 0.05) from either adults or neonates on scatterplots of control samples again demonstrated higher expression in neonatal cells under control conditions (Figure 3C). We therefore hypothesized that the higher baseline expression of LPS-activated genes in neonates might lead to reduced fold-change in many LPS-activated genes in neonates. Of the 1119 upregulated genes in adults and 669 upregulated genes in neonates, 480 were shared (Figure 3D). Examination of LPS-activated transcripts in control samples showed that the majority of genes activated by LPS in either adult or neonatal AMs had either similar expression under control conditions or higher expression in control neonates (Figure 3E). A small minority of LPS-activated genes were expressed higher in adults at baseline. Specific examples of genes are highlighted in Figure 3F. LPS induced high levels of inflammatory mediators, exemplified by *Il1b*, *Il6*, *Tnf*, and *Ccl3*, in both neonatal and adult cells. While these genes exhibited similar expression level after LPS, elevated basal expression in neonatal cells resulted in a lower LPS-activated fold change compared to adult cells. Among the genes exclusively induced in adult AMs, the expression levels of *Ikbke*, *S100a8*, and *Irf5* in neonatal cells at baseline were comparable to LPS-activated adult cells. High expression in control AMs was also observed for majority of genes uniquely upregulated in neonatal cells. Collectively, these data demonstrate

that neonatal AMs can mount robust innate immune response to LPS in vivo, with the most notable differences compared to adults being due to higher expression of inflammatory genes under control conditions.

Intranasal LPS Rapidly Reprograms the AM Chromatin Landscape In Vivo

We next tested if in vivo innate immune activation causes unique changes in the regulatory landscape of adult and neonatal AMs. After intranasal LPS stimulation, we performed ATAC-seq on isolated AMs. LPS caused rapid changes to the chromatin landscape in both adults and neonates (Figure S2E). Figure 4A illustrates examples of ATAC-seq peaks that exhibited overlapping changes in the open chromatin pattern after LPS exposure. Strongly induced pro-inflammatory genes, such as *Il1b*, *Ccl4*, and *Nfkbia*, exhibited a dramatic increase in ATAC-seq peak amplitude, consistent with LPS-induced changes in chromatin structure. Genome-wide comparison of open chromatin regions between LPS treated and control AMs identified around 800 to 1000 genomics sites with differentially accessible chromatin in adults and neonates (Figure 4B). In contrast, comparison of LPS samples between adults and neonates revealed slightly fewer than 200 differentially open chromatin sites. While 93 peaks were specific to LPS treated adult AMs, 78 peaks were specific to LPS treated neonatal AMs (Figure 4C). These results demonstrate conserved chromatin dynamics in activated adult and neonatal AMs.

We next performed de novo motif analysis on genomic sites that gained ATAC-seq peaks after LPS activation. In both adults and neonates, the analysis returned motifs assigned to NF-κB and AP-1 family members. Compared to adult cells, these motifs were more significantly enriched in neonatal cells (Figure 4D). To infer probable TFs responsible for

induction of inflammatory response in each AMs, we measured gene expression of highly expressed family members that recognize the enriched motifs. Adult and neonatal AMs exposed to LPS exhibited largely similar expression pattern. Expression of AP-1 family members were sensitive to LPS in both adult and neonatal AMs. Similarly, members of the NF-κB family, *Nfkb1*, *Nfkb2*, *Relb*, and *Rel* were all upregulated and expressed at comparable levels between adult and neonatal cells after LPS (Figure 4E). Collectively, these results show that adult and neonatal AMs use similar canonical regulatory mechanisms in mediating the in vivo innate immune response upon TLR activation.

The Lung Microenvironment Drives Unique Transcriptional Signatures in Adult and Neonatal AMs

Adult and neonatal AMs expressed unique transcriptional profiles but had relatively conserved core innate immune responses. We questioned whether the differences in gene expression under control conditions, in particular the pro-inflammatory signature measured in neonatal AMs, was due to inherent developmental programs or differences in the adult and neonatal lung microenvironments. Tissue specific microenvironments instruct macrophage phenotypes in different organs, but the impact of development and age on environmental effects are unclear. To test the influence of microenvironment in driving AM identity, we first measured expression of several known AM signature genes following isolation and culturing of adult AMs in vitro. Interestingly, expression of the pan-macrophage marker *Spi1* (encoding PU.1) remained consistent in culture, while expression of more specific AM genes (*Pparg* and *Car4*) rapidly fell following removal from the lung (Figure 5A). We next used RNA-seq to measure how the adult and neonatal lung microenvironment might direct global AM

24

transcriptional programs. PCA analysis illustrated how 20 h of culture altered overall transcription in both neonatal and adult cells (Figure 5B). The transition into culture reduced expression of many AM genes (Figure 5C). In addition, the divergent transcriptional profiles between adult and neonatal AMs converged following removal from the lung microenvironment (Figure 5D). The heat-map visualization in Figure 5E highlights genes specific to adult or neonatal cells that were highly sensitive to environmental change. The expression of nearly half of the adult-specific genes was altered in culture (Figure 5F), whereas changing the microenvironment only altered about 10% of genes shared in common between adult and neonatal AMs. Similar effects were measured in genes enriched in neonatal AMs. Metascape analysis indicated that removing adult cells from the lung microenvironment downregulated genes related to fatty acid metabolism that were enriched in vivo (Figure 5G). Most of the enriched pathways in neonatal AMs were also sensitive to removal from the lung, particularly those involved in tissue morphogenesis and vascular development. However, Metascape categories related to inflammatory response and cytokine production were notably not impacted by culturing neonatal AMs. These results suggested that the adult and neonatal lung microenvironments are required for many of the unique transcriptional differences between the different developmental stages. However, a component of the proinflammatory signature in neonatal AM appears to not be environmentally sensitive.

Environmental Impact on AM Chromatin Landscapes

To investigate how the lung microenvironment might regulate AM-specific transcription, we first examined AM TF expression from our RNA-seq dataset. Expression of the pan-macrophage factor *Spi1* was maintained in culture, albeit reduced in cultured neonatal

25

AMs (Figure 6A). However, expression of *Pparg*, *Cebpb*, and *Atf5* were are reduced in cultured cells, consistent with the lung microenvironment being required for expression of AM-specific TFs. We next tested the impact of the in vivo lung microenvironment in regulating innate immune function. Adult and neonatal AMs were stimulated with LPS either immediately after isolation or after placement in tissue culture. For both adults and neonates, longer culture times enhanced the cytokine expression in LPS-treated AMs (Figure 6B). As basal cytokine expression did not increase in culture, these results suggest that both adult and neonatal lung microenvironments actively work to temper innate immune inflammatory responses without making AMs unresponsive.

To better understand how the lung microenvironment might regulate innate immune response, we examined expression of key TFs involved in macrophage function and immune response. In adult cells, KLF family members and the nuclear receptor *Nr3c1* were reduced by in vitro culture (Figure 6C). In neonates, IRF and NF-κB family members increased, whereas most AP-1 family members were downregulated. These data suggested that the lung microenvironment was required for expression of key TFs regulating AM function and components of the innate immune response. Next, we performed ATAC-seq to analyze accessible regions of chromatin in the vicinity of genes that exhibited reduced expression in vitro to link these environmental influences to the epigenetic landscape. In both adult and neonatal cells, de novo motif analysis identified loss of motifs recognized by PU.1, CEBP, and KLF factors following removal from the lung (Figure 6D). In addition to these common motifs, the analysis also recovered motifs specific for each cell. For example, ATAC-seq peaks associated with downregulated genes in Adult AMs were enriched for MITF and ATF motifs. In neonatal AMs, NFIL3 and AP-1 were top motifs associated with reduced expression in

26

culture. Figure 6E illustrates examples of ATAC-seq peaks that exhibit substantial reduction in the vicinity of downregulated genes after culturing. Overall, these data emphasize the critical role of environment in establishing gene regulatory landscapes unique to adult and neonatal AMs.

DISCUSSION

Here we investigated the transcriptomes and chromatin landscapes to identify the molecular features differentiating AMs from adult and neonatal mouse lungs. The unique transcriptional and chromatin patterns within each time point were likely associated with specialized AM roles in lung development and homeostasis. Adult AMs were enriched for genes associated with fatty acid metabolism and signaling, consistent with their role in recycling and metabolism the massive amounts of lipid contained within lung surfactant. Neonatal AMs were enriched in genes related to tissue morphogenesis and vascular development, reflecting the dynamics of alveolar development during the neonatal period in mice (25, 33). While the specific roles of AM in alveolar formation have not been clearly demonstrated, tissue macrophages have been implicated in vascular remodeling, removal of apoptotic cells, and paracrine interactions with lung epithelial cells (31, 34, 35). Therefore, we speculate that neonatal AMs may play important roles in lung development.

Our data demonstrated a constitutive pro-inflammatory phenotype in neonatal AMs compared to adult AMs. Neonatal cells expressed higher level of inflammatory transcripts (*Il1b, Il6, Tnf, and S100a8*) enriched with binding motifs for AP1, NF-κB, and IRF. Higher basal levels of genes subsequently increased by in vivo LPS exposure suggested a pre-activated or primed inflammatory state in neonatal AMs. As a marker for this pro-inflammatory signature, *Il1b* expression increased during late gestation, peaked at birth, and decreased following birth into adulthood. These findings are consistent with previous work demonstrating that fetal liver-derived macrophages exhibited a pro-inflammatory phenotype within fetal liver and lung tissues compared to yolk sac-derived macrophages (85). The role of this pro-inflammatory phenotype in balancing immune tolerance and protection against pathogens at birth is not yet

28

clear. A newborn lung containing primed AMs may provide protection against microbes but could also lead to exaggerated and uncontrolled inflammation, especially in infants born preterm. Recent data from human preterm infants requiring mechanical ventilation has in fact drawn connections between inflammatory gene expression in AM around the time of birth and more severe chronic lung disease (86).

Both adult and neonatal AMs mounted a robust innate immune response in vivo when challenged with intranasal LPS. RNA-seq and ATAC-seq data demonstrated activation of genes containing motifs for the canonical innate immune TFs AP-1 and NF-κB. Neonatal AMs did display some unique features in gene expression following LPS activation, including a smaller number of DE genes compared to LPS-treated adult AMs. Reduced induction of proinflammatory cytokines, such as *Il1b*, *Il6*, and *Tnf*, in neonatal cells, are suggestive of an immunocompromised or tolerant state in newborns (3, 38, 87, 88). However, we found the actual gene expression level after LPS treatment was comparable between adult and neonatal AMs, with the elevated basal expression levels in neonatal cells leading to a reduced LPS-activated fold change. We therefore suggest a more global context is necessary in determining whether or not the innate immune response of newborns is truly deficient when compared to adults.

Culturing isolated macrophages ex vivo immediately alters their transcriptional program. At present, tissue-derived signals that regulate AM phenotype and functions from neonatal and adult lungs remain largely unknown. Our novel LPS inhalation model emphasizes the importance of conducting experiments in vivo to capture innate immune response of AMs within unique microenvironment of neonatal and adult lungs.

The lung microenvironment was required for the unique transcriptional profiles of both neonatal and adult AMs. Transferring isolated AMs to a cell culture environment led to profound and rapid changes in gene expression. While the expression of the pan-macrophage marker *Spi1* and genes shared between neonatal and adult AMs held constant, cell culture quickly reduced expression of AM signature genes and many of the differentially expressed genes between adult and neonatal AMs. These data suggested the lung microenvironment contains signals required for establishing the unique AM identity at each developmental age. Intriguingly, the inflammatory phenotype of neonatal AMs was partially conserved in culture. While cell culture reduced expression of most AP-1 members in neonatal AMs, expression of IRF and NF-κB persisted. Together, these results implicate both inherent and environmentally-sensitive mechanisms in differentiating neonatal and adult AMs.

Our findings add another layer to the current knowledge on the developmental program of AM identity and functions. We postulate that proinflammatory, primed AM precursors migrate from the liver to the lung in the developing fetus. Once in the lung, the inflammatory phenotype persists as these macrophages differentiate into more mature AM in the days following delivery. Additional factors such as developmental regulation of cell surface receptors may further regulate tolerance or immune activation in these immature myeloid populations (29). We propose changes in the lung environment around the time of birth further promote expression of inflammatory genes in AM precursors. The dramatic changes at birth, including clearance of amniotic fluid, initiation of breathing and exposure to oxygen, and inhalation of commensal and pathogenic microbes, could each drive inflammatory gene expression. Production of lipid-rich surfactant could then gradually instruct differentiated AMs to acquire a more tolerant quiescent baseline phenotype without compromising their response

to innate immune stimuli. In addition to surfactant, epithelial IL-10 and TGF-β likely each promote this quiescent phenotype in adult AMs. Further identification of the molecular mechanisms regulating adult and neonatal immune states could further our understanding of lung injury, repair, and regeneration in a variety of disease states across the lifespan.

Acknowledgements

Figure 1. Unique Transcriptional Signatures Differentiate Adult and Neonatal AMs

(A) Flow cytometry analysis and AM isolation gating strategy from adult and neonatal lungs.

(B) Scatter plot of RNA-seq data comparing adult and neonatal AMs. Differentially expressed genes selected using <u>limma</u> ($Log_2FC > 1$, p-adj < 0.05). Genes significantly up-regulated in adult and neonatal AMs are highlighted in black and red, respectively. Data shown here are from three independent experiments with four biological replicates.

(C) Scatter plot of RNA-seq data comparing adult and neonatal AMs. AM-specific genes defined by Gautier et al. (2012) (82) are color-coded in brown.

(D) Bar plots for expression (counts per million [CPM]) of AM signature genes and classical monocyte genes in Asterisks represents statistical significance **p-adj < 0.01 and ***p-adj < 0.001 calculated from limma. Error bars, SD.

(E) Metascape analysis of top 12 enriched pathways in adult and neonatal AMs. Analysis performed on differentially expressed genes between adult and neonatal AMs ($Log_2FC > 1$, p-adj < 0.05).

(F) Bar plots for expression (CPM) of representative genes in adult and neonatal AMs from the Metascape analysis. Asterisks represents statistical significance, **p-adj < 0.01 and ***p-adj < 0.001 calculated from limma. Error bars, SD.
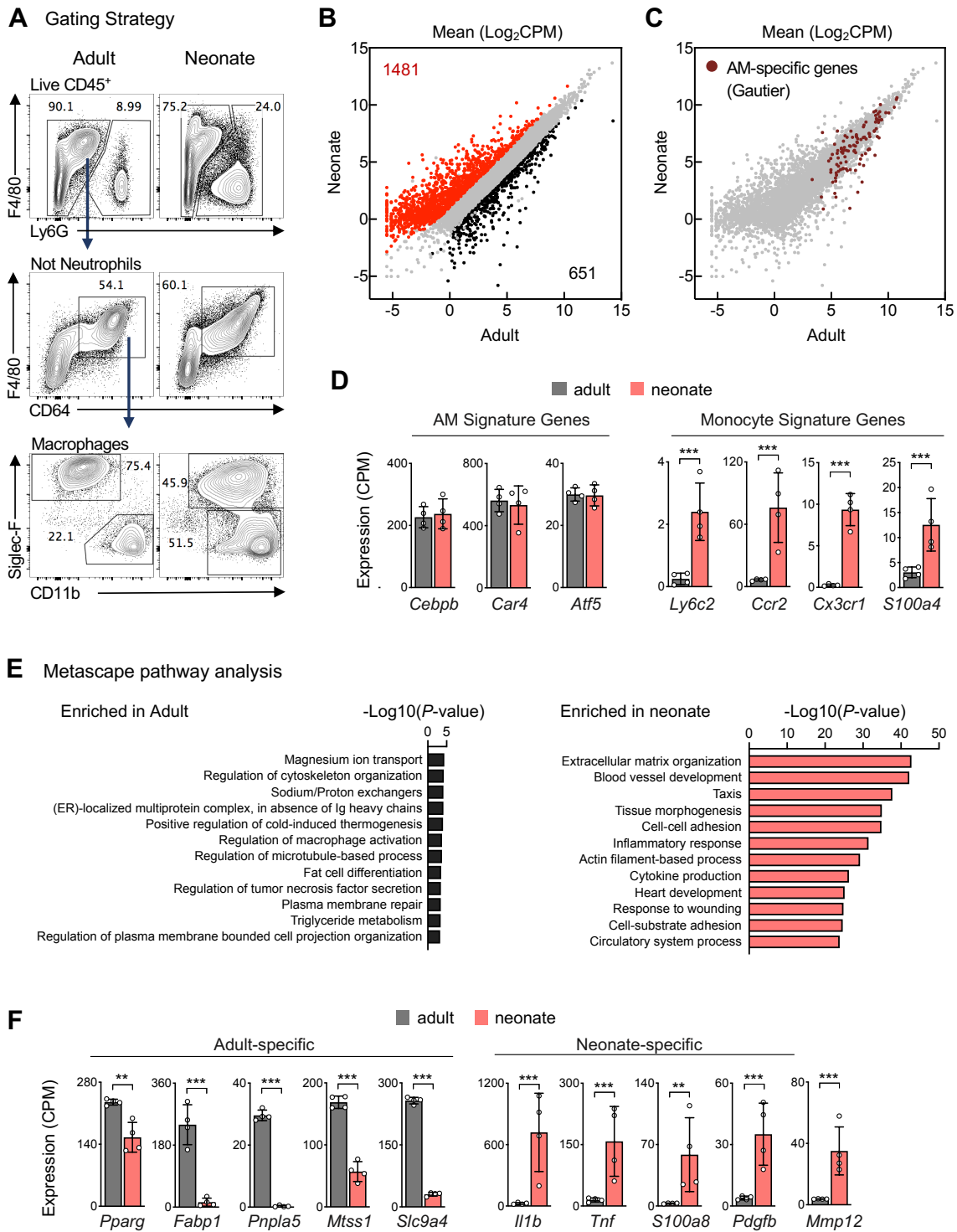
Figure 1. Unique Transcriptional Signatures Differentiate Adult and Neonatal AMs

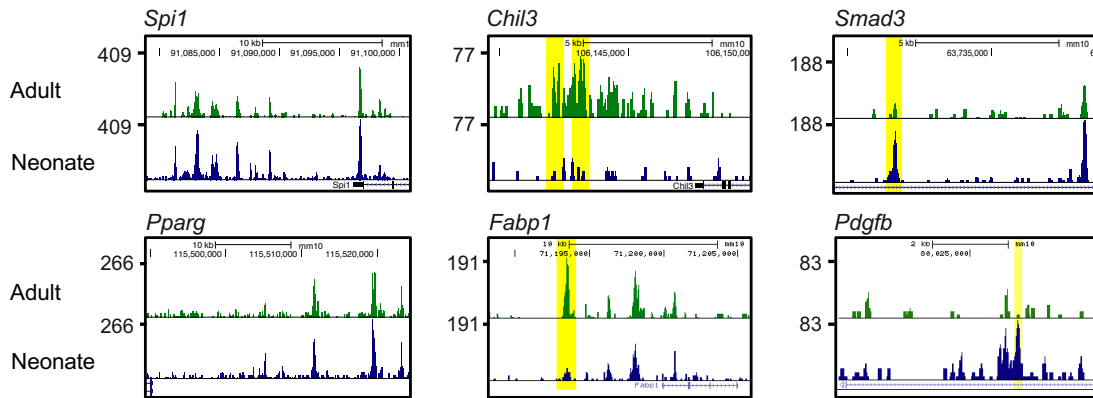**Figure 2. Distinct Transcriptional Regulators Inferred from Open Chromatin Profiles**
(A) Genome browser tracks of ATAC-seq peaks in the vicinity of the indicated genes in adult and neonatal AMs. Yellow shading highlights accessible chromatin regions unique to either adult or neonatal AMs.
(B) Scatterplot illustrating genome-wide comparison of irreproducibility discovery rate (IDR)-defined distal ATAC-seq peak tag counts (distance from TSS > 2kb) between neonatal and adult AMs. Chromatin regions with significantly more open in adults and neonates ($Log_2FC >$ 1, p-adj < 0.05) are color coded in green and blue, respectively. Data shown here are IDR peaks from two biological replicates.
(C) Homer *de novo* motif enrichment analysis of distal accessible chromatin regions specific to adult and neonatal AMs. Analysis performed on adult or neonate AM-specific ATAC-seq peaks using neonate or adult AMs ATAC-seq peaks as a background, respectively.
(D, E) Heatmap of highly expressed TF family members (above 16 CPM in at least one sample) recognizing motifs identified in Figure 2C and S1D.

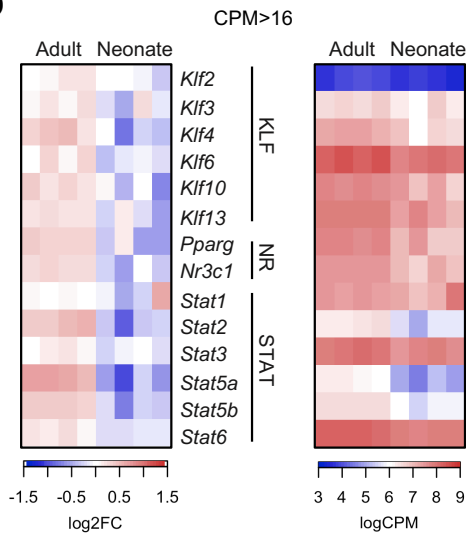**A** Examples of ATAC-seq browser tracks

Spi1 · *Chil3* · *Smad3* · *Pparg* · *Fabp1* · *Pdgfb*

B ATAC-seq (log2(tag counts+1))
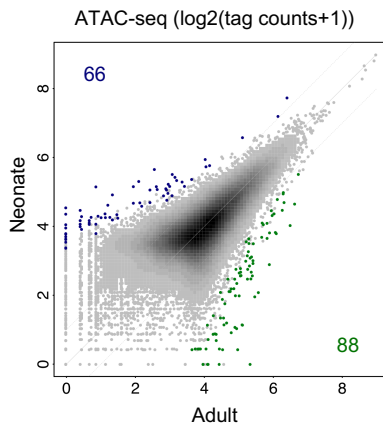
C De novo motifs

Motif	*P*-val	Adult (%) / Neonate (%)	Best Match
	1e-28	39.53/4.28	KLF
	1e-24	29.07/0.95	GR (NR)
	1e-18	30.23/3.23	STAT

Motif	*P*-val	Neonate (%) / Adult (%)	Best Match
	1e-20	28.79/1.56	IRF
	1e-20	28.79/2.17	AP-1
	1e-15	30.30/3.36	NF-κB

D CPM>16
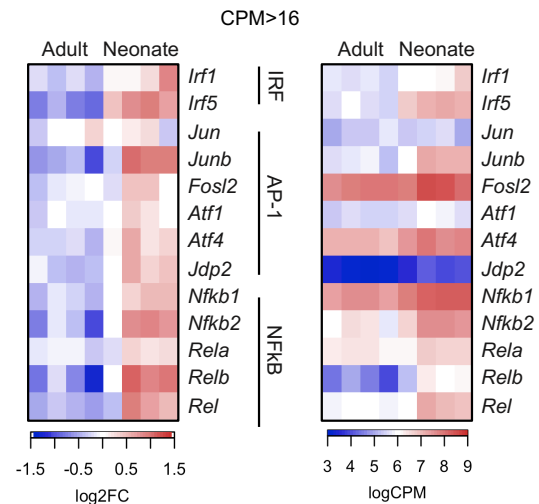
E CPM>16

Figure 2. Distinct Transcriptional Regulators Inferred from Open Chromatin Profiles

35

Figure 3. LPS Induces Robust Innate Immune Response in Adult and Neonatal AMs In Vivo

(A) Scatter plot of RNA-seq data comparing AMs, 2 h after i.n. instillation of PBS (control) or LPS, from neonatal and adult lungs. Differentially expressed genes selected using limma ($Log_2FC > 1$, p-adj < 0.05). Genes significantly up-regulated and down-regulated following LPS in adult AMs are in green and black, respectively and in neonatal AMs are in red and black. Data shown here are from three independent experiments with four biological replicates.

(B) (Top) IPA functional analysis of genes differentially expressed ($Log_2FC > 1$, p-adj < 0.05) between LPS and PBS samples for each adult and neonatal AMs. Bar graphs represent the activation z-score for a selection of significantly enriched canonical pathways that are either activated (positive z-score) or inhibited (negative z-score) following LPS instillation. (Bottom) IPA functional analysis of genes differentially expressed ($Log_2FC > 1$, p-adj < 0.05) between PBS samples of adult and neonatal AMs. Gray and pink bars represent significantly enriched pathways activated in adult AMs (positive z-score) and neonatal AMs (negative z-score), respectively.

(C) Scatter plot of RNA-seq data comparing adult and neonatal AMs under control conditions for genes activated ($Log_2FC > 2$, p-adj < 0.05) following LPS instillation. Data shown here are from three independent experiments with four biological replicates.

(D) Venn diagram illustrating genes upregulated or downregulated after 2 h of i.n. LPS instillation in neonatal AMs versus adult AMs.

(E) Pie chart depicting baseline expression of genes upregulated in both neonatal and adult AMs, exclusively in adult AMs, or neonatal AMs after i.n. LPS instillation from Figure 3D.
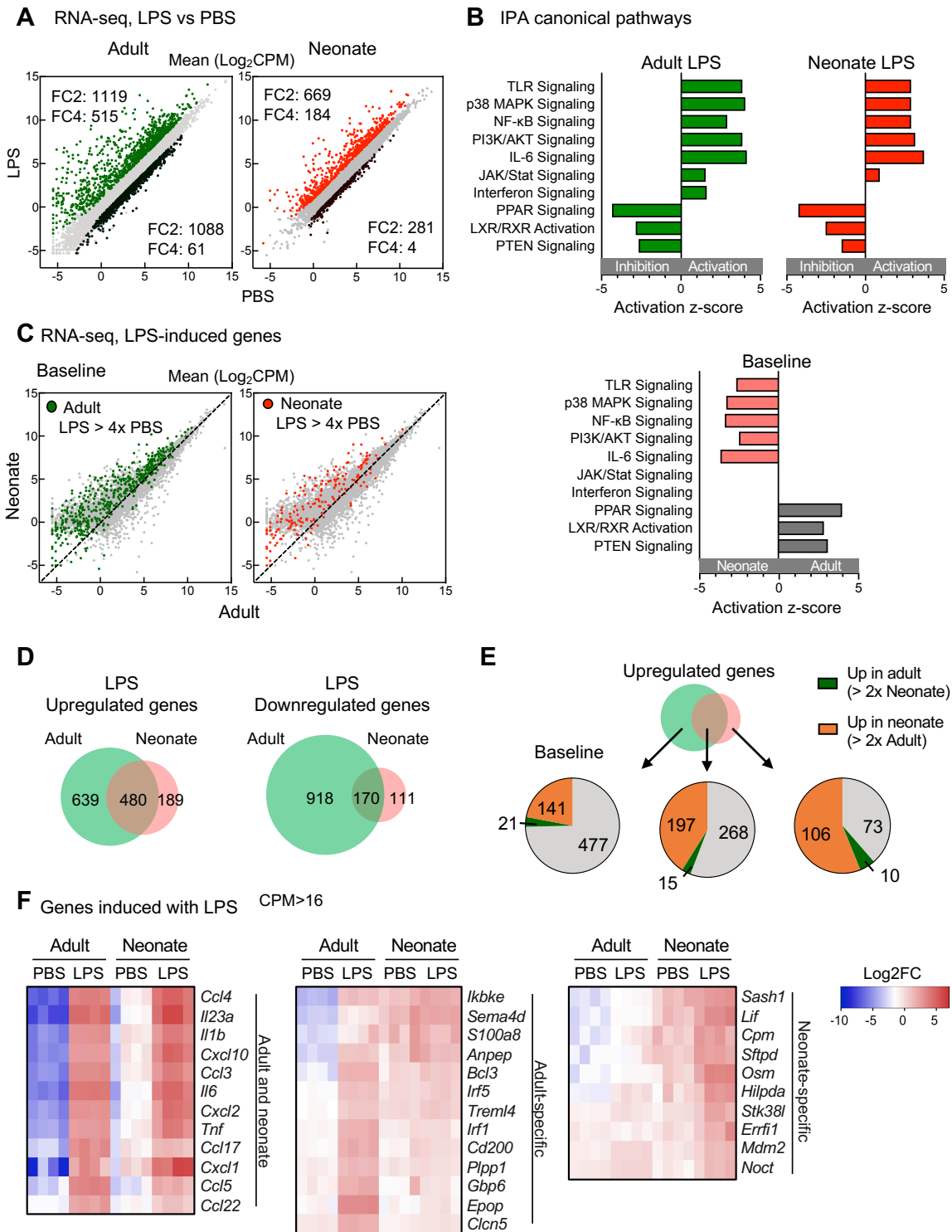
(F) Heatmap of representative genes from Figure 3E.

Figure 3. LPS Induces Robust Innate Immune Response in Adult and Neonatal AMs In Vivo

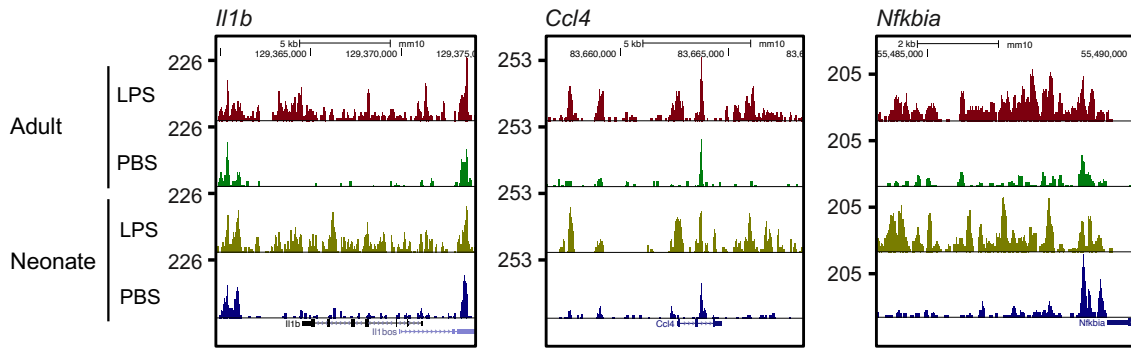**Figure 4. Intranasal LPS rapidly reprograms the AM chromatin landscape in vivo**

(A) Genome browser tracks of ATAC-seq peaks in the vicinity of the indicated genes activated in adult and neonatal AMs at 2 h following LPS instillation.

(B, C) Scatterplot illustrating genome-wide comparison of IDR-defined distal ATAC-seq peak tag counts (distance from TSS > 2kb) between (B) PBS and LPS samples for each adult and neonatal AMs and (C) LPS samples of adult and neonatal AMs. Data shown here are IDR peaks from two biological replicates.

(D) De novo motifs enriched at distal accessible chromatin regions of LPS samples compared to PBS samples for each neonatal and adult AMs.

(E) Heatmap of highly expressed TF family members (above 16 CPM in at least one sample) recognizing motifs identified in Figure 4D.
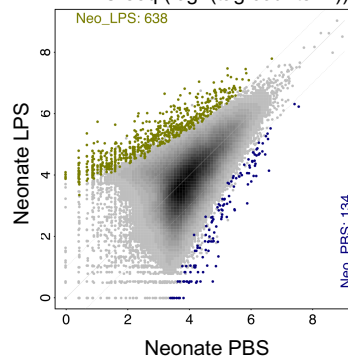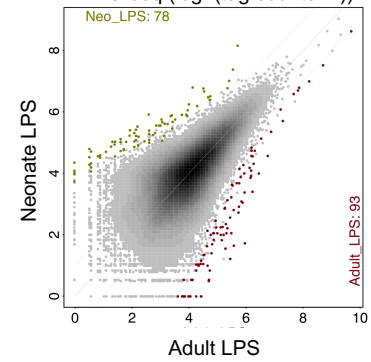
A Examples of ATAC-seq browser tracks
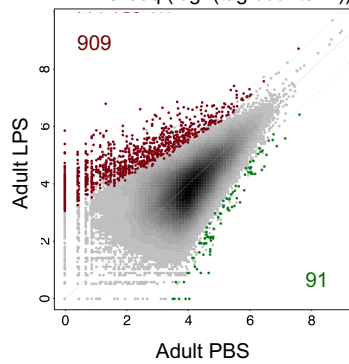
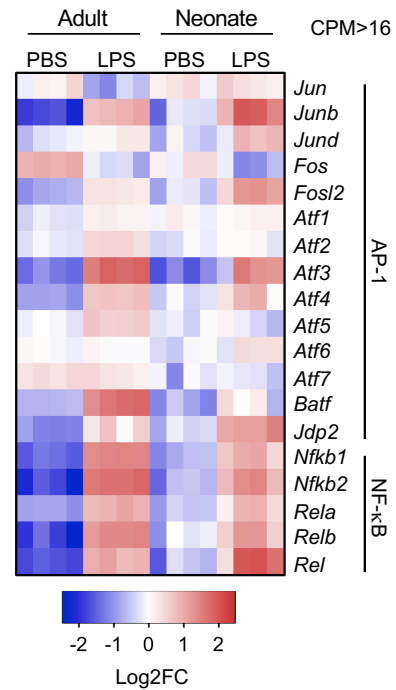**Figure 4.** Intranasal LPS rapidly reprograms the AM chromatin landscape in vivo

39
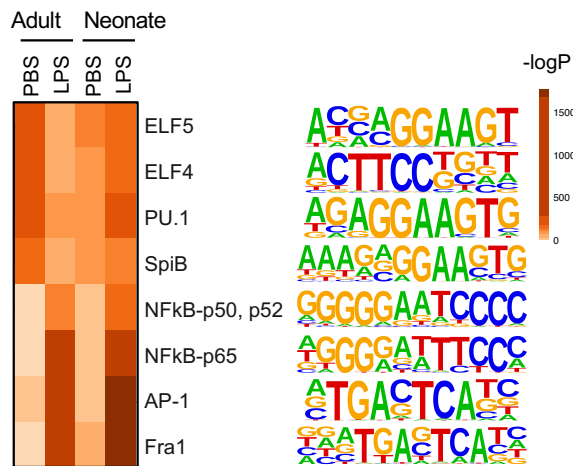
Figure 5. The Lung Microenvironment Drives Unique Transcriptional Signatures of Adult and Neonatal AMs

(A) Real time PCR analysis of macrophage and AM signature genes in adult AMs after transfer to culture environment in the presence of M-CSF from 0 to 20h. Asterisks represents statistical significance **p-adj < 0.01, ***p-adj < 0.001. Data shown here are from three biological replicates.

(B) PCA of the 12,149 detectable genes in freshly isolated neonatal and adult AMs and after maintenance in culture with M-CSF for 20h. Data shown here are from two independent experiments with three biological replicates.

(C) Scatter plot of RNA-seq data illustrating effects of culture environment on AM-specific genes defined by (dark red) for each adult and neonatal AMs. AM-specific genes defined by Gautier et al. (2012) (82) are color-coded in brown.

(D) Scatter plot of RNA-seq data illustrating the effect of culture environment in the presence of M-CSF for 20h on differentially expression genes ($Log_2FC > 2$, p-adj < 0.05) between neonatal and adult AMs. Genes significantly up-regulated in neonatal and adult AMs are highlighted in red and black, respectively. Data shown here are from two independent experiments with three biological replicates.

(E) Heatmap illustrating changes in expression of adult-specific or neonatal specific genes ($Log_2FC > 1$, p-adj < 0.05), 20 hours after transfer to culture environment.

(F) Pie chart depicting the effect of culture environment on (top) adult-specific ($Log_2FC > 1$, p-adj < 0.05) or common mRNAs ($Log_2FC < +/- 0.5$, p-adj < 0.05) in adult AMs or on (bottom) neonatal-specific or common mRNAs in neonatal AMs.

(G) Metascape analysis depicting the effects of culture environment on top 12 pathways enriched under control conditions of neonatal and adult AMs from Figure 1C.
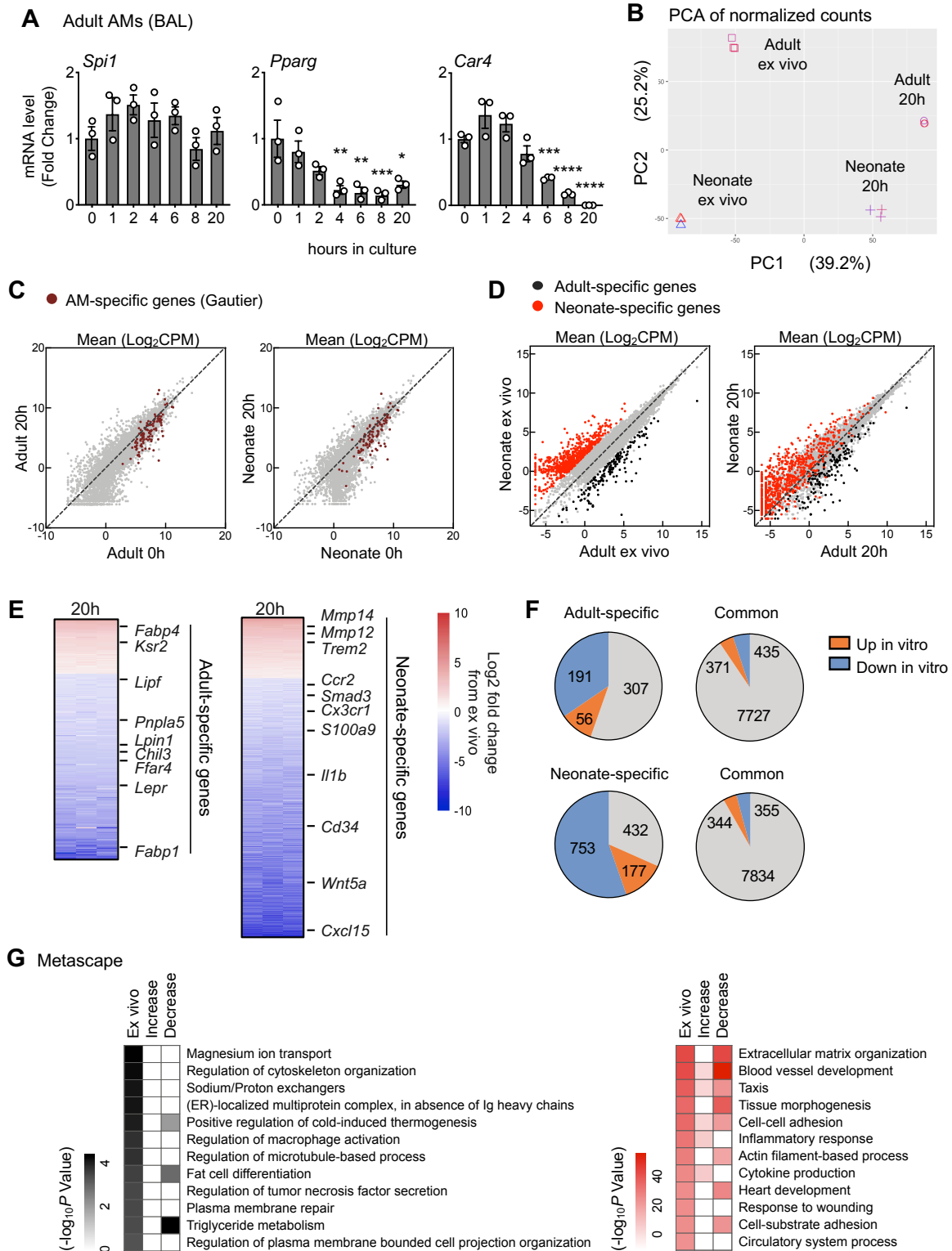
Figure 5. The Lung Microenvironment Drives Unique Transcriptional Signatures of Adult and Neonatal AMs

Figure 6. Environmental Impact on AM Chromatin Landscapes

(A) Bar plots for expression of key TFs for macrophage lineage and AM development in neonatal and adult AMs 20 h after transfer to culture environment in the presence of M-CSF. Asterisks represents statistical significance ***p-adj < 0.001 calculated from limma. Error bars, SD.

(B) Real time PCR analysis of *Il1b* and *Il6* mRNA expression in adult and neonatal AMs treated with LPS for 2 h either immediate after isolation or after 10-20 h of tissue culture. Data shown here are from three biological replicates.

(C) Heatmap illustrating the effect of culture environment on expression of TF family members (above 16 CPM in at least one sample) recognizing motifs identified in Figure 2B and Figure S1D

(D) Heatmap illustrating the effect of culture environment on expression of TF family members recognizing motifs identified in Figure 2B and S1F.

(E) Genome browser tracks of ATAC-seq peaks in the vicinity of the indicated genes in adult and neonatal AMs.
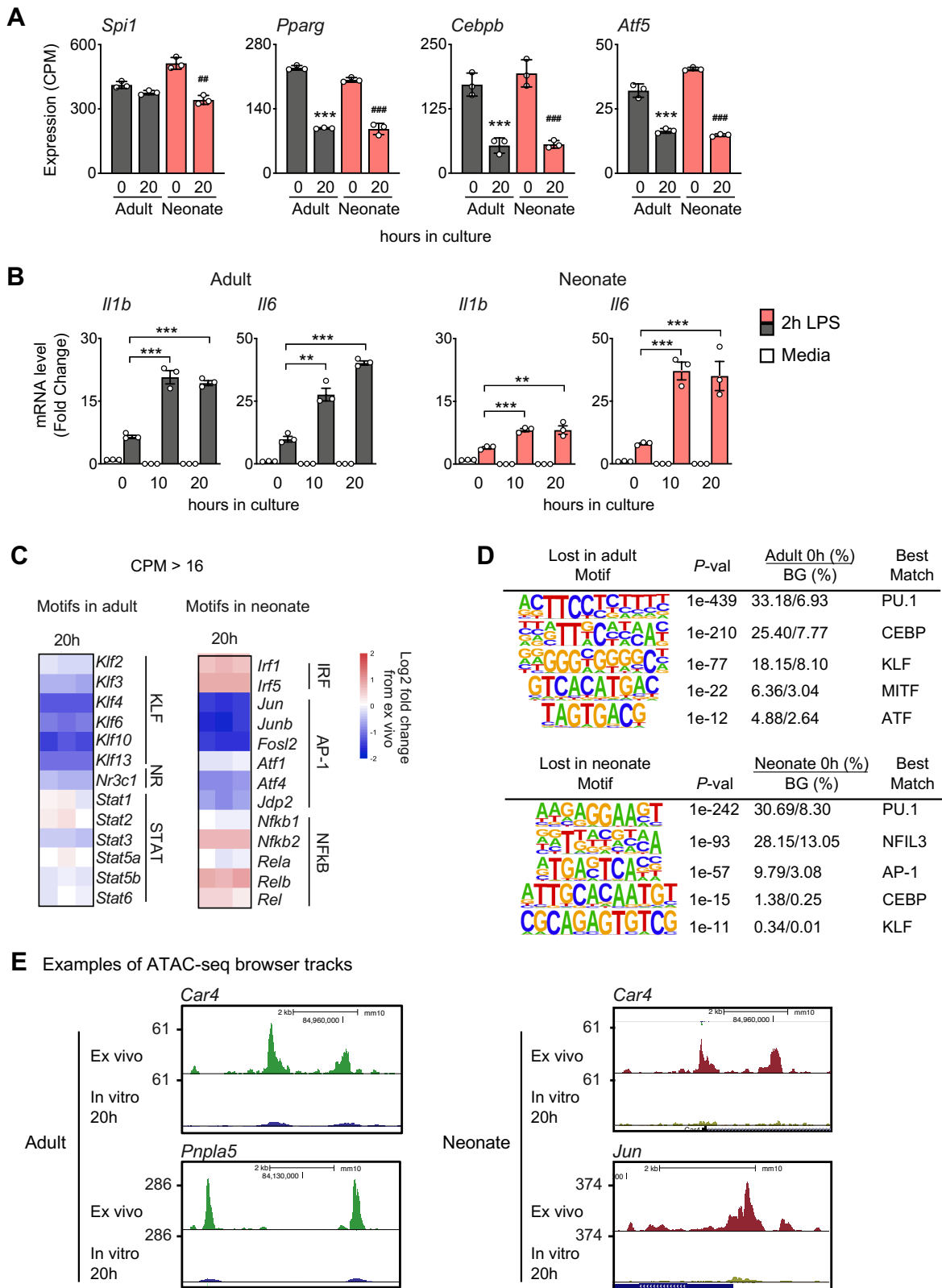
Figure 6. Environmental Impact on AM Chromatin Landscapes

Figure S1. Supplement to Figure 1 and 2

(A) PCA of 12,195 detectable genes in adult and neonatal AMs AMs following 2 h exposure of either PBS or LPS administered i.n.

(B) IPA functional analysis of genes differentially expressed (Log$_2$FC > 1, p-adj < 0.05) between adult and neonatal AMs. Bar graphs show a selection of highly significant canonical pathways and their activation z-score. Gray and pink bars represent significantly enriched pathways activated in adult AMs (positive z-score) and neonatal AMs (negative z-score), respectively.

(C) Real time PCR analysis *Il1b* mRNA expression in fetal monocyte, pre-AMs, or AMs. Data shown here are from three biological replicates.

(D) Homer known motif enrichment analysis of distal accessible chromatin regions specific to adult and neonatal AMs using all peaks as a background.

(E) Heatmap of highly expressed TF family members (above 16 CPM in at least one sample) recognizing motifs identified in Figure S1D.

A PCA of normalized counts

B IPA canonical pathways

C

D Known Motifs

Motif	P-val	Target (%) BG (%)	Best Match
AGAGGAAGTG	1e-102	31.06/5.96	PU.1
TGGGTGTGGC	1e-23	29.90/15.48	KLF
TGACCTTTGCCCCA	1e-9	18.56/11.15	PPARG

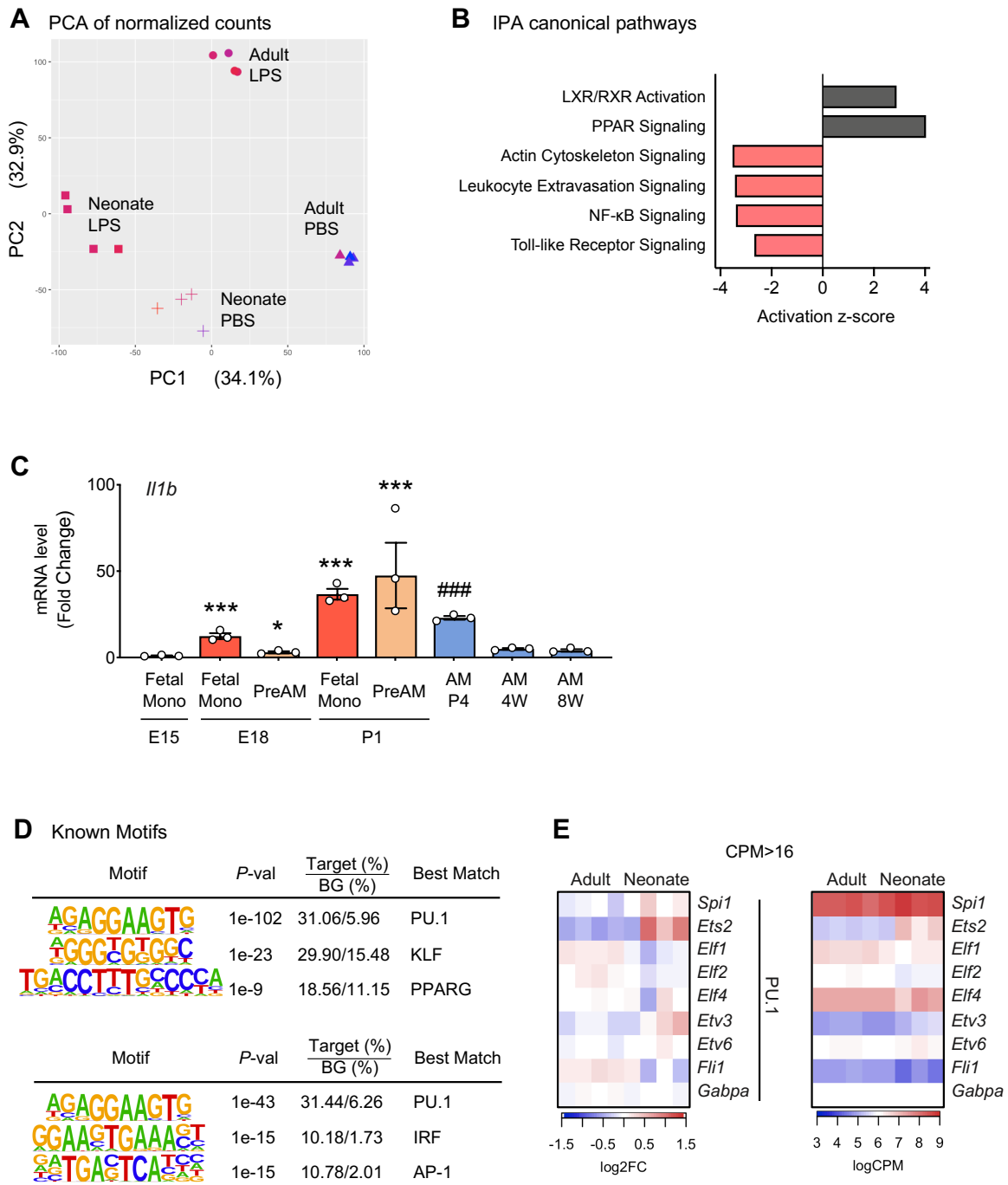| Motif	P-val	Target (%) BG (%)	Best Match
AGAGGAAGTG	1e-43	31.44/6.26	PU.1
GGAAGTGAAAGT	1e-15	10.18/1.73	IRF
GATGACTCATCC	1e-15	10.78/2.01	AP-1

E

Figure S1. Supplement to Figure 1 and 2

45

Figure S2. Supplement to Figure 3 and 4

(A) Flow cytometry analysis of lung neutrophils and macrophage subpopulations after i.n. LPS instillation. Bar graphs represent the average percentage of each cell subset out of CD45$^+$ leukocytes.

(B, C) (B) Flow cytometry analysis of macrophage populations for intracellular Pro-IL1β expression 2 h following i.n. PBS or LPS instillation (C) Bar graphs represent the average percentage of Pro-IL1β$^+$ out of each cell subset.

(D) Metascape analysis of genes upregulated after 2 h of i.n. LPS instillation compared with PBS treated control (Log$_2$FC > 1, p-adj < 0.05) in each adult and neonatal AMs. Bar graphs represent top 12 enriched pathways.

(E) Heatmap of open chromatin regions defined by ATAC-seq in adult and neonatal AMs following 2 h of PBS and LPS instillation i.n. Data are from two biological replicates.
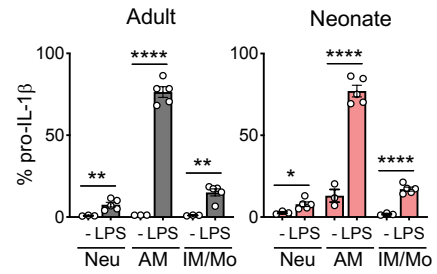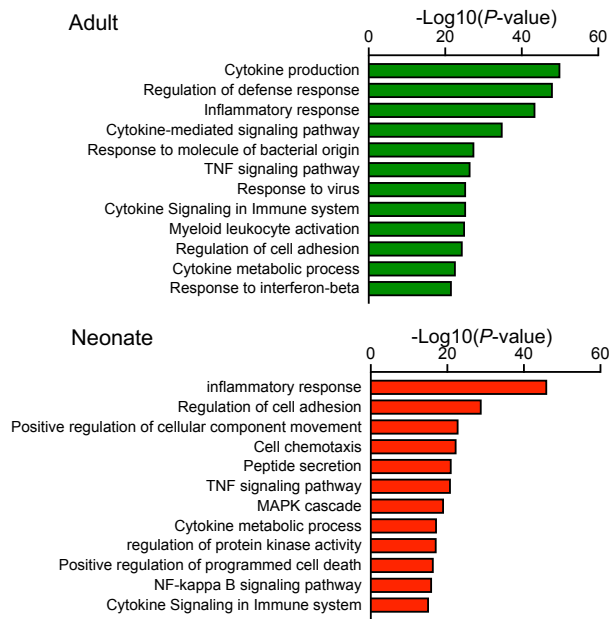
A Percentages, i.n. LPS
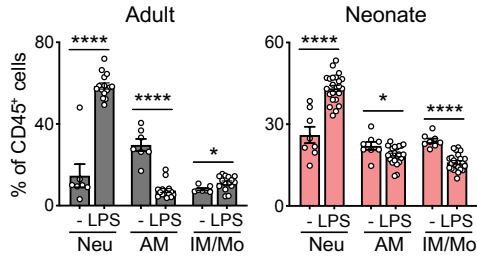
B FACS Analysis, pro-IL-1β⁺ cells
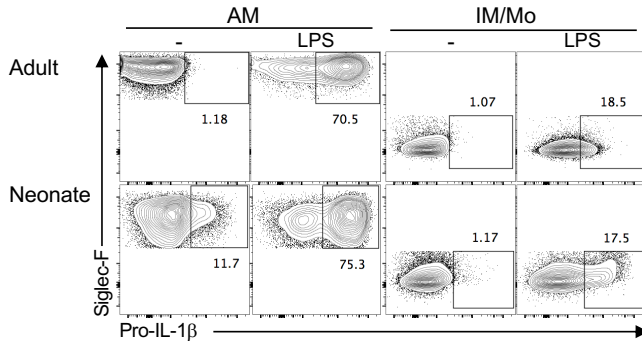
C Percentages, pro-IL-1β⁺ cells

D Metascape: LPS Upregulated
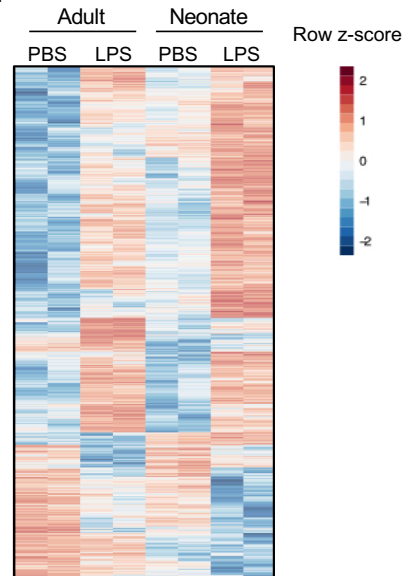
E

Figure S2. Supplement to Figure 3 and 4

REFERENCES

1.   Shiffman J. Issue attention in global health: the case of newborn survival. *Lancet.* 2010;375(9730):2045-9.

2.   Brady MT. Health care–associated infections in the neonatal intensive care unit. *American journal of infection control.* 2005;33(5):268-75.

3.   Levy O. Innate immunity of the newborn: basic mechanisms and clinical correlates. *Nature Reviews Immunology.* 2007;7(5):379-90.

4.   Reiterer F. Neonatal pneumonia. *Neonatal bacterial infection.* 2013:19-32.

5.   Wilson CB, Nizet V, Maldonado Y, Remington JS, and Klein JO. *Remington and Klein's infectious diseases of the fetus and newborn infant.* Elsevier Health Sciences; 2015.

6.   Chmielarczyk A, Wójkowska-Mach J, Romaniszyn D, Adamski P, Helwich E, Lauterbach R, Pobiega M, Borszewska-Kornacka M, Gulczyńska E, and Kordek A. Mode of delivery and other risk factors for Escherichia coli infections in very low birth weight infants. *BMC pediatrics.* 2014;14(1):274.

7.   Barton L, Hodgman JE, and Pavlova Z. Causes of death in the extremely low birth weight infant. *Pediatrics.* 1999;103(2):446-51.

8.   Shahzad T, Radajewski S, Chao C-M, Bellusci S, and Ehrhardt H. Pathogenesis of bronchopulmonary dysplasia: when inflammation meets organ development. *Molecular and Cellular Pediatrics.* 2016;3(1):23.

9.   D'Angio CT, Ambalavanan N, Carlo WA, McDonald SA, Skogstrand K, Hougaard DM, Shankaran S, Goldberg RN, Ehrenkranz RA, and Tyson JE. Blood cytokine profiles associated with distinct patterns of bronchopulmonary dysplasia among extremely low birth weight infants. *The Journal of pediatrics.* 2016;174:45-51. e5.

10.   Lal CV, and Ambalavanan N. Biomarkers, early diagnosis, and clinical predictors of bronchopulmonary dysplasia. *Clinics in perinatology.* 2015;42(4):739-54.

11.   Savani RC. *Seminars in perinatology*. Elsevier; 2018:459-70.

12.   Stoll BJ, Hansen NI, Bell EF, Shankaran S, Laptook AR, Walsh MC, Hale EC, Newman NS, Schibler K, Carlo WA, Kennedy KA, Poindexter BB, Finer NN, Ehrenkranz RA, Duara S, Sanchez PJ, O'Shea TM, Goldberg RN, Van Meurs KP, Faix RG, Phelps DL, Frantz ID, 3rd, Watterberg KL, Saha S, Das A, Higgins RD, Eunice Kennedy Shriver National Institute of Child H, and Human Development Neonatal Research N. Neonatal outcomes of extremely preterm infants from the NICHD Neonatal Research Network. *Pediatrics.* 2010;126(3):443-56.

13.   Husain AN, Siddiqui NH, and Stocker JT. Pathology of arrested acinar development in postsurfactant bronchopulmonary dysplasia. *Human pathology.* 1998;29(7):710-7.

14.   MARGRAF LR, Tomashefski Jr JF, Bruce MC, and Dahms BB. Morphometric Analysis of the Lung in Bronchopulmonary Dysplasia1-3. *Am Rev Respir Dis.* 1991;143:391-400.

15.   Jobe AH. *Seminars in neonatology.* Elsevier; 2003:9-17.

16.   Tullus K, Noack GW, Burman LG, Nilsson R, Wretlind B, and Brauner A. Elevated cytokine levels in tracheobronchial aspirate fluids from ventilator treated neonates with bronchopulmonary dysplasia. *Eur J Pediatr.* 1996;155(2):112-6.

17.   Jonsson B, Tullus K, Brauner A, Lu Y, and Noack G. Early increase of TNF alpha and IL-6 in tracheobronchial aspirate fluid indicator of subsequent chronic lung disease in preterm infants. *Arch Dis Child Fetal Neonatal Ed.* 1997;77(3):F198-201.

18.   D'Angio CT, Ambalavanan N, Carlo WA, McDonald SA, Skogstrand K, Hougaard DM, Shankaran S, Goldberg RN, Ehrenkranz RA, Tyson JE, Stoll BJ, Das A, Higgins RD, Eunice Kennedy Shriver National Institute of Child H, and Human Development Neonatal Research N. Blood Cytokine Profiles Associated with Distinct Patterns of Bronchopulmonary Dysplasia among Extremely Low Birth Weight Infants. *J Pediatr.* 2016;174:45-51 e5.

19.   Benjamin JT, Carver BJ, Plosa EJ, Yamamoto Y, Miller JD, Liu J-H, van der Meer R, Blackwell TS, and Prince LS. NF-κB activation limits airway branching through inhibition of Sp1-mediated fibroblast growth factor-10 expression. *The Journal of Immunology.* 2010;185(8):4896-903.

20.   Smith VC, Zupancic JAF, McCormick MC, Croen LA, Greene J, Escobar GJ, and Richardson DK. Rehospitalization in the first year of life among infants with bronchopulmonary dysplasia. *J Pediatr-Us.* 2004;144(6):799-803.

21.   Doyle LW, Faber B, Callanan C, Freezer N, Ford GW, and Davis NM. Bronchopulmonary dysplasia in very low birth weight subjects and lung function in late adolescence. *Pediatrics.* 2006;118(1):108-13.

22.   Hussell T, and Bell TJ. Alveolar macrophages: plasticity in a tissue-specific context. *Nature reviews immunology.* 2014;14(2):81-93.

23.   Kopf M, Schneider C, and Nobs SP. The development and function of lung-resident macrophages and dendritic cells. *Nature immunology.* 2015;16(1):36-44.

24.   Elliott MR, and Ravichandran KS. Clearance of apoptotic cells: implications in health and disease. *Journal of Cell Biology.* 2010;189(7):1059-70.

25.   Whitsett JA, Wert SE, and Weaver TE. Alveolar surfactant homeostasis and the pathogenesis of pulmonary disease. *Annual review of medicine.* 2010;61:105-19.

26.   Blackwell TS, Hipps AN, Yamamoto Y, Han W, Barham WJ, Ostrowski MC, Yull FE, and Prince LS. NF-κB signaling in fetal lung macrophages disrupts airway morphogenesis. *The Journal of Immunology.* 2011;187(5):2740-7.

27.   Stouch AN, McCoy AM, Greer RM, Lakhdari O, Yull FE, Blackwell TS, Hoffman HM, and Prince LS. IL-1β and inflammasome activity link inflammation to abnormal fetal airway development. *The Journal of Immunology.* 2016;196(8):3411-20.

28.   Kalymbetova TV, Selvakumar B, Rodríguez‑Castillo JA, Gunjak M, Malainou C, Heindl MR, Moiseenko A, Chao CM, Vadász I, and Mayer K. Resident alveolar macrophages are master regulators of arrested alveolarization in experimental bronchopulmonary dysplasia. *The Journal of Pathology.* 2018;245(2):153-9.

29.   Lund SJ, Patras KA, Kimmey JM, Yamamura A, Butcher LD, Del Rosario PG, Hernandez GE, McCoy AM, Lakhdari O, and Nizet V. Developmental Immaturity of Siglec Receptor Expression on Neonatal Alveolar Macrophages Predisposes to Severe Group B Streptococcal Infection. *Iscience.* 2020;23(6).

30.   Metzger RJ, Klein OD, Martin GR, and Krasnow MA. The branching programme of mouse lung development. *Nature.* 2008;453(7196):745-50.

31.   Morrisey EE, and Hogan BL. Preparing for the first breath: genetic and cellular mechanisms in lung development. *Developmental cell.* 2010;18(1):8-23.

32.   Kollmann TR, Kampmann B, Mazmanian SK, Marchant A, and Levy O. Protecting the newborn and young infant from infectious diseases: lessons from immune ontogeny. *Immunity.* 2017;46(3):350-63.

33.   Desai TJ, Brownfield DG, and Krasnow MA. Alveolar progenitor and stem cells in lung development, renewal and cancer. *Nature.* 2014;507(7491):190-4.

34.   Hashimoto S, Nakano H, Singh G, and Katyal S. Elsevier; 2002.

35.   Lu MM, Li S, Yang H, and Morrisey EE. Foxp4: a novel member of the Foxp subfamily of winged-helix genes co-expressed with Foxp1 and Foxp2 in pulmonary and gut tissues. *Mechanisms of development.* 2002;119:S197-S202.

36.   Guilliams M, De Kleer I, Henri S, Post S, Vanhoutte L, De Prijck S, Deswarte K, Malissen B, Hammad H, and Lambrecht BN. Alveolar macrophages develop from fetal monocytes that differentiate into long-lived cells in the first week of life via GM-CSF. *Journal of Experimental Medicine.* 2013;210(10):1977-92.

37.   Hillman NH, Kallapur SG, and Jobe AH. Physiology of transition from intrauterine to extrauterine life. *Clinics in perinatology.* 2012;39(4):769-83.

38.   Kollmann TR, Levy O, Montgomery RR, and Goriely S. Innate immune function by Toll-like receptors: distinct responses in newborns and the elderly. *Immunity.* 2012;37(5):771-83.

39.   Basha S, Surendran N, and Pichichero M. Immune responses in neonates. *Expert review of clinical immunology.* 2014;10(9):1171-84.

40.   Harbeson D, Ben-Othman R, Amenyogbe N, and Kollmann TR. Outgrowing the immaturity myth: the cost of defending from neonatal infectious disease. *Frontiers in immunology.* 2018;9:1077.

41.   Schulz C, Perdiguero EG, Chorro L, Szabo-Rogers H, Cagnard N, Kierdorf K, Prinz M, Wu B, Jacobsen SEW, and Pollard JW. A lineage of myeloid cells independent of Myb and hematopoietic stem cells. *Science.* 2012;336(6077):86-90.

42.   Ginhoux F, and Guilliams M. Tissue-resident macrophage ontogeny and homeostasis. *Immunity.* 2016;44(3):439-49.

43.   Epelman S, Lavine KJ, and Randolph GJ. Origin and functions of tissue macrophages. *Immunity.* 2014;41(1):21-35.

44.   Ginhoux F, Greter M, Leboeuf M, Nandi S, See P, Gokhan S, Mehler MF, Conway SJ, Ng LG, and Stanley ER. Fate mapping analysis reveals that adult microglia derive from primitive macrophages. *Science.* 2010;330(6005):841-5.

45.   Schneider C, Nobs SP, Kurrer M, Rehrauer H, Thiele C, and Kopf M. Induction of the nuclear receptor PPAR-γ by the cytokine GM-CSF is critical for the differentiation of fetal monocytes into alveolar macrophages. *Nature immunology.* 2014;15(11):1026-37.

46.   Yu X, Buttgereit A, Lelios I, Utz SG, Cansever D, Becher B, and Greter M. The cytokine TGF-β promotes the development and homeostasis of alveolar macrophages. *Immunity.* 2017;47(5):903-12. e4.

47.   Hashimoto D, Chow A, Noizat C, Teo P, Beasley MB, Leboeuf M, Becker CD, See P, Price J, and Lucas D. Tissue-resident macrophages self-maintain locally throughout adult life with minimal contribution from circulating monocytes. *Immunity.* 2013;38(4):792-804.

48.   Lavin Y, Winter D, Blecher-Gonen R, David E, Keren-Shaul H, Merad M, Jung S, and Amit I. Tissue-resident macrophage enhancer landscapes are shaped by the local microenvironment. *Cell.* 2014;159(6):1312-26.

49.   Okabe Y, and Medzhitov R. Tissue-specific signals control reversible program of localization and functional polarization of macrophages. *Cell.* 2014;157(4):832-44.

50.	Gosselin D, Link VM, Romanoski CE, Fonseca GJ, Eichenfield DZ, Spann NJ, Stender JD, Chun HB, Garner H, and Geissmann F. Environment drives selection and function of enhancers controlling tissue-specific macrophage identities. *Cell.* 2014;159(6):1327-40.

51.	van de Laar L, Saelens W, De Prijck S, Martens L, Scott CL, Van Isterdael G, Hoffmann E, Beyaert R, Saeys Y, and Lambrecht BN. Yolk sac macrophages, fetal liver, and adult monocytes can colonize an empty niche and develop into functional tissue-resident macrophages. *Immunity.* 2016;44(4):755-68.

52.	Gosselin D, Skola D, Coufal NG, Holtman IR, Schlachetzki JC, Sajti E, Jaeger BN, O'Connor C, Fitzpatrick C, and Pasillas MP. An environment-dependent transcriptional network specifies human microglia identity. *Science.* 2017;356(6344).

53.	Izquierdo HM, Brandi P, Gómez M-J, Conde-Garrosa R, Priego E, Enamorado M, Martínez-Cano S, Sánchez I, Conejero L, and Jimenez-Carretero D. Von hippel-lindau protein is required for optimal alveolar macrophage terminal differentiation, self-renewal, and function. *Cell reports.* 2018;24(7):1738-46.

54.	Zhang W, Li Q, Li D, Li J, Aki D, and Liu Y-C. The E3 ligase VHL controls alveolar macrophage function via metabolic–epigenetic regulation. *Journal of Experimental Medicine.* 2018;215(12):3180-93.

55.	Eddy WE, Gong K-Q, Bell B, Parks WC, Ziegler SF, and Manicone AM. Stat5 is required for CD103+ dendritic cell and alveolar macrophage development and protection from lung injury. *The Journal of Immunology.* 2017;198(12):4813-22.

56.	Cain DW, O'Koren EG, Kan MJ, Womble M, Sempowski GD, Hopper K, Gunn MD, and Kelsoe G. Identification of a tissue-specific, C/EBPβ-dependent pathway of differentiation for murine peritoneal macrophages. *The Journal of Immunology.* 2013;191(9):4665-75.

57.	Sinclair C, Bommakanti G, Gardinassi L, Loebbermann J, Johnson MJ, Hakimpour P, Hagan T, Benitez L, Todor A, and Machiah D. mTOR regulates metabolic adaptation of APCs in the lung and controls the outcome of allergic inflammation. *Science.* 2017;357(6355):1014-21.

58.	Nakamura A, Ebina-Shibuya R, Itoh-Nakadai A, Muto A, Shima H, Saigusa D, Aoki J, Ebina M, Nukiwa T, and Igarashi K. Transcription repressor Bach2 is required for pulmonary surfactant homeostasis and alveolar macrophage function. *Journal of Experimental Medicine.* 2013;210(11):2191-204.

59.	Gross DS, and Garrard WT. Nuclease hypersensitive sites in chromatin. *Annual review of biochemistry.* 1988;57(1):159-97.

60.	Heinz S, Benner C, Spann N, Bertolino E, Lin YC, Laslo P, Cheng JX, Murre C, Singh H, and Glass CK. Simple combinations of lineage-determining transcription

factors prime cis-regulatory elements required for macrophage and B cell identities. *Molecular cell.* 2010;38(4):576-89.

61.   Ostuni R, Piccolo V, Barozzi I, Polletti S, Termanini A, Bonifacio S, Curina A, Prosperini E, Ghisletti S, and Natoli G. Latent enhancers activated by stimulation in differentiated cells. *Cell.* 2013;152(1-2):157-71.

62.   Glass CK, and Natoli G. Molecular control of activation and priming in macrophages. *Nature immunology.* 2016;17(1):26-33.

63.   Ghisletti S, Barozzi I, Mietton F, Polletti S, De Santa F, Venturini E, Gregory L, Lonie L, Chew A, and Wei C-L. Identification and characterization of enhancers controlling the inflammatory gene expression program in macrophages. *Immunity.* 2010;32(3):317-28.

64.   Heinz S, Romanoski C, Benner C, Allison K, Kaikkonen M, Orozco L, and Glass C. Effect of natural genetic variation on enhancer selection and function. *Nature.* 2013;503(7477):487-92.

65.   Kaikkonen MU, Spann NJ, Heinz S, Romanoski CE, Allison KA, Stender JD, Chun HB, Tough DF, Prinjha RK, and Benner C. Remodeling of the enhancer landscape during macrophage activation is coupled to enhancer transcription. *Molecular cell.* 2013;51(3):310-25.

66.   Barish GD, Ruth TY, Karunasiri M, Ocampo CB, Dixon J, Benner C, Dent AL, Tangirala RK, and Evans RM. Bcl-6 and NF-κB cistromes mediate opposing regulation of the innate immune response. *Genes & development.* 2010;24(24):2760-5.

67.   Andrews S. Babraham Bioinformatics, Babraham Institute, Cambridge, United Kingdom; 2010.

68.   Bolger AM, Lohse M, and Usadel B. Trimmomatic: a flexible trimmer for Illumina sequence data. *Bioinformatics.* 2014;30(15):2114-20.

69.   Dobin A, Davis CA, Schlesinger F, Drenkow J, Zaleski C, Jha S, Batut P, Chaisson M, and Gingeras TR. STAR: ultrafast universal RNA-seq aligner. *Bioinformatics.* 2013;29(1):15-21.

70.   Li B, and Dewey CN. RSEM: accurate transcript quantification from RNA-Seq data with or without a reference genome. *BMC bioinformatics.* 2011;12(1):323.

71.   Frankish A, Diekhans M, Ferreira A-M, Johnson R, Jungreis I, Loveland J, Mudge JM, Sisu C, Wright J, and Armstrong J. GENCODE reference annotation for the human and mouse genomes. *Nucleic acids research.* 2019;47(D1):D766-D73.

72.   Robinson MD, and Oshlack A. A scaling normalization method for differential expression analysis of RNA-seq data. *Genome biology.* 2010;11(3):1-9.

73.   Benjamini Y, and Hochberg Y. Controlling the false discovery rate: a practical and powerful approach to multiple testing. *Journal of the Royal statistical society: series B (Methodological).* 1995;57(1):289-300.

74.   Zhang B, Kirov S, and Snoddy J. WebGestalt: an integrated system for exploring gene sets in various biological contexts. *Nucleic acids research.* 2005;33(suppl_2):W741-W8.

75.   Subramanian A, Tamayo P, Mootha VK, Mukherjee S, Ebert BL, Gillette MA, Paulovich A, Pomeroy SL, Golub TR, and Lander ES. Gene set enrichment analysis: a knowledge-based approach for interpreting genome-wide expression profiles. *Proceedings of the National Academy of Sciences.* 2005;102(43):15545-50.

76.   Hänzelmann S, Castelo R, and Guinney J. GSVA: gene set variation analysis for microarray and RNA-seq data. *BMC bioinformatics.* 2013;14(1):7.

77.   Tarca AL, Draghici S, Khatri P, Hassan SS, Mittal P, Kim J-s, Kim CJ, Kusanovic JP, and Romero R. A novel signaling pathway impact analysis. *Bioinformatics.* 2009;25(1):75-82.

78.   Langmead B, and Salzberg SL. Fast gapped-read alignment with Bowtie 2. *Nature methods.* 2012;9(4):357.

79.   Li Q, Brown JB, Huang H, and Bickel PJ. Measuring reproducibility of high-throughput experiments. *The annals of applied statistics.* 2011;5(3):1752-79.

80.   Love MI, Huber W, and Anders S. Moderated estimation of fold change and dispersion for RNA-seq data with DESeq2. *Genome biology.* 2014;15(12):550.

81.   Kent WJ, Sugnet CW, Furey TS, Roskin KM, Pringle TH, Zahler AM, and Haussler D. The human genome browser at UCSC. *Genome research.* 2002;12(6):996-1006.

82.   Gautier EL, Shay T, Miller J, Greter M, Jakubzick C, Ivanov S, Helft J, Chow A, Elpek KG, and Gordonov S. Gene-expression profiles and transcriptional regulatory pathways that underlie the identity and diversity of mouse tissue macrophages. *Nature immunology.* 2012;13(11):1118-28.

83.   Gordon S. Alternative activation of macrophages. *Nature reviews immunology.* 2003;3(1):23-35.

84.   Mass E, Ballesteros I, Farlik M, Halbritter F, Günther P, Crozet L, Jacome-Galarza CE, Händler K, Klughammer J, and Kobayashi Y. Specification of tissue-resident macrophages during organogenesis. *Science.* 2016;353(6304).

85.   Lakhdari O, Yamamura A, Hernandez GE, Anderson KK, Lund SJ, Oppong-Nonterah GO, Hoffman HM, and Prince LS. Differential Immune Activation in Fetal Macrophage Populations. *Sci Rep.* 2019;9(1):7677.

86. Sahoo D, Zaramela LS, Hernandez GE, Mai U, Taheri S, Dang D, Stouch AN, Medal RM, McCoy AM, and Aschner JL. Transcriptional profiling of lung macrophages identifies a predictive signature for inflammatory lung disease in preterm infants. *Communications biology.* 2020;3(1):1-12.

87. Dowling DJ, and Levy O. Ontogeny of early life immunity. *Trends in immunology.* 2014;35(7):299-310.

88. PrabhuDas M, Adkins B, Gans H, King C, Levy O, Ramilo O, and Siegrist C-A. Challenges in infant immunity: implications for responses to infection and vaccines. *Nature immunology.* 2011;12(3):189-94.